

On CAD/CAM generated fixed dental prostheses, fit and effect of ceramic veneering

Per Svanborg

Department of Prosthodontics/Dental Materials Science
Institute of Odontology
Sahlgrenska Academy at University of Gothenburg



UNIVERSITY OF GOTHENBURG

Gothenburg 2016

Cover illustration: Photo of CNC-milled CoCr FDP, by Per Svanborg

On CAD/CAM generated fixed dental prostheses, fit and effect of ceramic
veneering

© Per Svanborg 2016
per.svanborg@gu.se

ISBN 978-91-628-9949-3 (print)

<http://hdl.handle.net/2077/47406>

Printed in Gothenburg, Sweden 2016
Ineko

On CAD/CAM generated fixed dental prostheses, fit and effect of ceramic veneering

Per Svanborg

Department of Prosthodontics/Dental Materials Science, Institute of Odontology
Sahlgrenska Academy at University of Gothenburg
Göteborg, Sweden

ABSTRACT

The general aims of this thesis were to study CAD/CAM production processes, material aspects on cobalt-chromium (CoCr), clinical performance, and fit of tooth-, and implant-supported fixed dental prostheses (FDPs). A retrospective study of ceramic veneered CoCr FDPs was conducted to evaluate the performance of restorations made with the lost wax technique. One hundred forty-nine patients with 201 FDPs were followed for five years by data collection from patient records. To study CAD/CAM techniques, the fit of tooth-supported CNC-milled CoCr three-unit FDPs, made using conventional or digital impression techniques, was compared. Also, the fit of implant-supported CNC-milled and additively manufactured CoCr and titanium FDPs was evaluated before and after ceramic veneering.

CoCr FDPs are a promising alternative to other dental alloys, presenting a low level of ceramic fractures, cement failure, caries, and other complications during the first five years in function. To evaluate their longer-term success and possible biologic adverse effects, further long-term randomized controlled studies are necessary. The digital impression technique produced FDPs with a significantly more accurate fit than conventional impressions using VPS impression material. Implant-supported frameworks can be produced in either titanium or CoCr using either CNC-milling or additive manufacturing with a fit well within the range of what is regarded as clinically acceptable. The fit of frameworks of both materials and production techniques are affected by the ceramic veneering procedure to a small extent, most likely of no clinical significance.

Keywords: Metal ceramic alloys, Titanium, Cobalt, Chromium, Dental Marginal Adaptation, Dental Prosthesis, CAD, CAM, Tooth-Supported, Implant-Supported, Additive Manufacturing

ISBN: 978-91-628-9949-3 (print)

<http://hdl.handle.net/2077/47406>

ISBN: 978-91-628-9950-9 (PDF)

SAMMANFATTNING PÅ SVENSKA

Inom tandvården är användningen av kobolt-kromlegeringar för framställning av kronor och broar utbredd, trots att enbart ett fåtal kliniska studier har publicerats. De senaste åren har framställningstekniken för kobolt-krom förändrats, från formativ (gjutning) till subtraktiv (fräsning), vidare till additiv tillverkning (lasersmältning). För att digitalisera hela arbetsprocessen behöver även avtryckstagningen digitaliseras. Understrukturer av metall tillverkas ofta delvis med hjälp av digitala processer och täcks sedan med ett porslinslager för hand, för att ge den färdiga konstruktionen ett tandlikt utseende. Skillnaderna i termisk expansion mellan legeringen och porslinet kan påverka passformen negativt, framställningen kan ge inre spänningar i legeringen som eventuellt kan påverka passformen vid de höga temperaturer som bron utsätts för under porslinsbränningen.

Syftet med den här avhandlingen var att studera CAD/CAM framställningsmetoder, materialaspekter och klinisk överlevnad för metall keramiska broar i kobolt-krom, samt passformen på tand-, och implantatstödda brokonstruktioner. En studie av kobolt-krombroar med porslin gjordes för att utvärdera den kliniska överlevnaden på broar framställda med gjuttekniken. Etthundrafyrtionio patienter med 201 broar följdes i fem år retrospektivt genom att studera patientjournaler. För att studera CAD/CAM-tekniker så jämfördes passformen på frästa tandstödda tre-ledsbroar i kobolt-krom som framställdes med hjälp av konventionella eller digitala avtryck. Dessutom utvärderades passformen på frästa och additivt framställda implantatstödda kobolt-krom och titanbroar före och efter dessa genomgått porslinsbränning.

Kobolt-krombroar är ett lovande protetiskt alternativ till andra dentala legeringar, med få porslinsfrakturer, retentionsproblem, kariesangrepp, samt andra komplikationer under de fem första åren. För att kunna utvärdera funktion och en eventuell biologisk påverkan av kobolt-krom behövs fler kontrollerade, randomiserade kliniska långtidsuppföljningar. Den digitala avtryckstekniken visade lovande resultat med broar som hade statistiskt signifikant bättre passform jämfört med broar framställda med konventionell avtrycksteknik. När det gäller implantatstödda broar kan dessa framställas i både kobolt-krom och titan som material, de kan också framställas med både fräsning och additiv tillverkning med kliniskt jämförbar passform. Porslinsbränningen påverkade passformen på broar oberoende av material och framställningsteknik, men förändringen är troligen inte kliniskt märkbar.

LIST OF PAPERS

This thesis is based on the following studies, referred to in the text by their Roman numerals.

- I. Svanborg P, Långström L, Lundh R, Bjerkstig G, Örtorp A. A 5-year retrospective study of cobalt-chromium-based fixed dental prostheses. *Int J Prosthodont* 2013;26:343-349
- II. Svanborg P, Skjerven H, Carlsson P, Eliasson A, Karlsson S, Örtorp A. Marginal and internal fit of cobalt-chromium fixed dental prostheses generated from digital and conventional impressions. *Int J Dent* 2014:534382. doi: 10.1155/2014/534382.
- III. Svanborg P, Stenport V, Eliasson A. Fit of cobalt-chromium implant frameworks before and after ceramic veneering in comparison with CNC-milled titanium frameworks. *Clinical and Experimental Dental Research* 2015 doi: 10.1002/cre2.9
- IV. Svanborg P, Eliasson A, Stenport V. Additively manufactured titanium and cobalt-chromium implant frameworks, fit and effect of ceramic veneering. 2016 *Manuscript Submitted*

Paper I was reproduced with permission from Quintessence Publishing Co. Inc., Chicago, Illinois, USA.

CONTENT

ABBREVIATIONS	5
1 INTRODUCTION	6
1.1 Materials	8
1.1.1 Mechanical and physical properties of cobalt-chromium.....	8
1.1.2 Mechanical and physical properties of titanium.....	8
1.2 Biocompatibility.....	9
1.2.1 Cobalt-chromium.....	9
1.2.2 Titanium	10
1.3 Ceramic bond strength	11
1.3.1 Cobalt-chromium.....	11
1.3.2 Titanium	12
1.4 Production techniques	13
1.4.1 Formative manufacturing/Lost wax technique.....	13
1.4.2 Subtractive manufacturing/CNC-Milling.....	13
1.4.3 Additive manufacturing.....	14
1.5 Accuracy and precision	14
1.6 Tooth-supported FDPs	15
1.6.1 Fixed prostheses for prepared teeth.....	15
1.6.2 Techniques to measure fit.....	16
1.6.3 Impact of misfit	17
1.6.4 Fit of tooth-supported CoCr FDPs	18
1.7 Implant-supported FDPs	19
1.7.1 Prostheses for osseointegrated implants.....	19
1.7.2 Techniques to measure fit of implant-supported FDPs	20
1.7.3 Fit of implant-supported FDPs	21
1.7.4 Impact of misfit	21
1.8 Ceramic veneering of FDPs	22
2 BACKGROUND TO THE PRESENT THESIS	25

2.1	Design of the thesis	25
2.2	Aim	26
2.3	Specific aims	26
2.4	Hypotheses	27
3	MATERIAL AND METHODS	28
3.1	Part 1. Clinical study on tooth-supported CoCr FDPs (I).	28
3.1.1	Retrospective clinical study (I).....	28
3.1.2	Follow-up, dental records and radiographic examination	28
3.1.3	Patients.....	29
3.1.4	Definitions	29
3.1.5	Statistical analysis.....	30
3.2	Part 2. In vitro study on digital and conventional VPS impressions for tooth-supported FDPs (II).	30
3.2.1	Study casts	30
3.2.2	Conventional VPS impressions (control group).....	31
3.2.3	Digital impressions (test group).....	32
3.2.4	Fabrication of three-unit CoCr FDPs.....	33
3.2.5	Analysis of fit	33
3.2.6	Statistical analysis.....	34
3.3	Part 3. In vitro studies on the fit of CNC-milled and additively manufactured CoCr and Ti frameworks for implant-supported FDPs, and the effect of ceramic veneering (III-IV).....	35
3.3.1	Fabrication of master models and acrylic resin pattern	35
3.3.2	Fabrication of CoCr frameworks	35
3.3.3	Fabrication of Ti frameworks	36
3.3.4	Ceramic veneering of frameworks.....	36
3.3.5	Analysis of fit	38
3.3.6	Statistical analysis.....	39
4	RESULTS.....	41
4.1	Part 1. Clinical study on tooth-supported CoCr FDPs (I).	41
4.1.1	Follow-up.....	41

4.1.2 Patient Record Registrations	41
4.1.3 Failures According to Success/Survival Definitions	43
4.2 Part 2. In vitro study on digital and conventional VPS impressions for tooth-supported FDPs (II)	44
4.3 Part 3. In vitro studies on the fit of CNC-milled and additively manufactured CoCr and Ti frameworks for implant-supported FDPs, and the effect of ceramic veneering (III-IV).....	47
4.3.1 Fit results and comparisons within groups before and after ceramic veneering	47
4.3.2 Comparisons between groups.....	48
4.3.3 Ceramic veneering experiences.....	49
5 DISCUSSION	51
5.1 Discussion of materials and methods.....	51
5.1.1 Part 1. Clinical study on tooth-supported CoCr FDPs (I).	51
5.1.2 Part 2. In vitro study on digital and conventional VPS impressions for tooth-supported FDPs (II)	52
5.1.3 Part 3. In vitro studies on the fit of CNC-milled and additively manufactured CoCr and Ti frameworks for implant-supported FDPs, and the effect of ceramic veneering (III-IV).....	54
5.2 Discussion of results.....	56
5.2.1 Part 1. Clinical study on tooth-supported CoCr FDPs (I).	56
5.2.2 Part 2. In vitro study on digital and conventional VPS impressions for tooth-supported FDPs (II)	57
5.2.3 Part 3. In vitro studies on the fit of CNC-milled and additively manufactured CoCr and Ti frameworks for implant-supported FDPs, and the effect of ceramic veneering (III-IV).....	59
6 CONCLUSIONS.....	62
7 FUTURE PERSPECTIVES	63
ACKNOWLEDGEMENT	64
REFERENCES	65

ABBREVIATIONS

CoCr	Cobalt Chromium
CP Ti	Commercially Pure Titanium
TiAl6V4 ELI	Titanium, Aluminum 6%, Vanadium 4%, Extra Low Interstitial
FDP	Fixed Dental Prostheses
CAD/CAM	Computer Aided Design/Computer Aided Manufacturing
CNC	Computer Numeric Controlled
FEA	Finite Element Analysis
MC	Metal Ceramic
CTE	Coefficient of Thermal Expansion
AM	Additive Manufacturing
DLMS	Direct Laser Metal Sintering
SLS	Selective Laser Sintering
SLM	Selective Laser Melting
EBM	Electron Beam Melting
CMM	Coordinate Measuring Machine
SEM	Scanning Electron Microscopy
CSR	Cumulative Success/Survival Rate
VPS	Vinyl Poly Siloxane

1 INTRODUCTION

In dentistry, materials used historically for fixed prosthodontics have mainly consisted of gold-based (Au) alloys and palladium-silver (PdAg) alloys. Gold-based alloys were the primary choice for metal-ceramic (MC) restorations in fixed prosthodontics for more than 40 years. However, after the deregulation of the American gold standard in 1971, the price of gold increased and other high noble alloys like palladium-based alloys became more popular (1). Also, base metal alloys have been used in dentistry, as an alternative material for partial removable dentures, since 1928 (1) and during the 1970s, nickel-chromium (NiCr) and cobalt-chromium (CoCr) alloys were introduced and modified for use in fixed prosthodontics (2, 3). However, the usage of NiCr alloys has been questioned due to a potential biological response to nickel, and even CoCr alloys are being used despite the lack of studies regarding the clinical tolerance (4). In fixed prosthodontics, the material characteristics of CoCr are both positive and negative. The high solidus temperature makes CoCr suitable as a framework for ceramic veneers, and the difference from the ceramic sintering temperature minimizes the risk of framework distortion after sintering (3). Nevertheless, the high melting temperature and high coefficient of thermal expansion (CTE) may create problems in the dental laboratory since the high temperature is accompanied with an increased risk of technical difficulties (5). The high modulus of elasticity makes it possible to design frameworks with reduced thickness and longer pontic spans compared to conventional gold alloys. But the stiffness and hardness of the material makes it hard to cut, grind and polish in the laboratory and clinic. The potential difficulties in the handling of the lost wax technique for CoCr can to some extent be reduced by computer aided design/computer aided manufacturing (CAD/CAM) production sequences (6). The processes of fabricating a dental restoration are: impression of the oral situation, jaw, gums and teeth, design of the restoration and manufacturing of the restoration. The impression can be made using an impression tray and a silicone or polyether material or using an intraoral scanner (Digital impression). The design of the restoration can be done either using wax on a stone cast derived from the silicone impression, or in a CAD environment derived from the digital impression or a scan of the stone cast (Figure 1 & 2). The manufacturing of dental restorations in CoCr can be done using different production techniques, the traditional technique is the lost wax technique, a formative technique also called casting, but the lost wax technique is being rapidly replaced by CAD/CAM techniques in dentistry and dental technology (7). Today the CAD/CAM techniques dominate framework manufacturing in implant dentistry. The CAD/CAM techniques used in dentistry for the production of CoCr include both

subtractive and additive manufacturing (AM), such as computer numeric controlled (CNC) milling and laser melting, and the quality and fit of these restorations need to be evaluated (8).

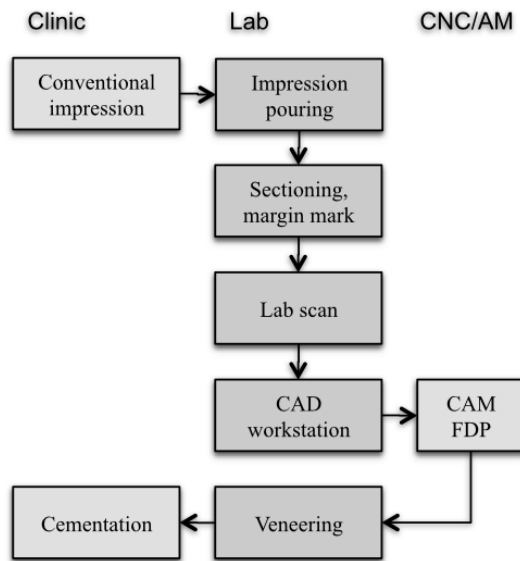


Figure 1. Example of workflow using conventional impression and lab scanning of stone cast.

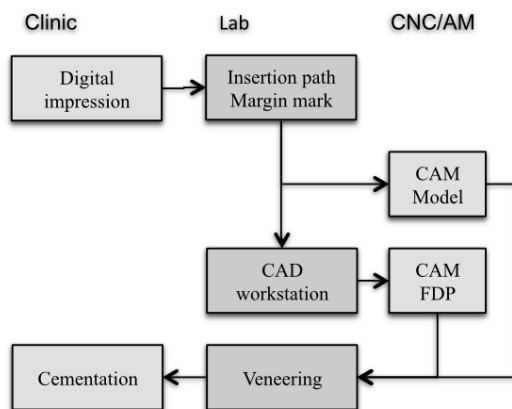


Figure 2. Example of workflow using digital impression.

1.1 Materials

1.1.1 Mechanical and physical properties of cobalt-chromium

The main constituent of CoCr alloys is cobalt with approximately 60 weight percent of the total content. Cobalt (Co) is a transition metal with atomic number 27. Cobalt has a hexagonal-close-packed (HCP) crystalline structure, which gives the material fewer slip planes than body-centered-cubic (BCC) and face-centered-cubic (FCC) structures. Chromium (Cr) is added to the alloy for strength and for its passivating abilities, to reduce the risk of corrosion. Other elements added to CoCr alloys are e.g. tungsten (W), molybdenum (Mo), silicon (Si) and manganese (Mn). This gives CoCr alloys material properties such as; low density, high melting temperature, high modulus of elasticity and hardness (1). Depending on the manufacturing technique, the alloys may have different elements and properties. In a study comparing the hardness of CoCr alloys manufactured by various techniques, it was concluded that AM CoCr had a Vickers hardness (HV) value of 371 ± 10 , cast CoCr had 320 ± 12 HV and CNC-milled CoCr had 297 ± 5 HV (9). In another study comparing cast and additively manufactured CoCr, it was found that the tensile strength and the yield strength were significantly higher for the AM CoCr (tensile strength 1307.5 ± 10.65 MPa, yield strength 884.37 ± 8.96 MPa) compared to the strength of cast CoCr (tensile strength 758.37 ± 25.85 MPa, yield strength 568.10 ± 30.94 MPa) (10).

According to a finite element analysis (FEA) study by Sertgoz, rigid materials should be chosen as superstructure for implant-supported FDPs, in order to reduce the risk of technical complications, such as retaining screw fracture (11). One of the most rigid material combinations available in implant dentistry today is CoCr with ceramic veneer, which has demonstrated clinical results (biological and technical complications) comparable to a Au alloy after 18 years of follow up (12). Few ceramic chippings were reported in studies on ceramic veneered CoCr tooth-supported FDPs and single crowns after five years (13, 14), indicating that the material combination may be suitable for clinical use from a technical viewpoint.

1.1.2 Mechanical and physical properties of titanium

In dentistry, both commercially pure (CP) and alloyed titanium (Ti) materials are used. The American society for testing and materials (ASTM) has classified CP-Ti in four grades by composition. All four grades have

approximately 99 % Ti, but with different amounts of impurity elements such as, iron (Fe), carbon (C), hydrogen (H), nitrogen (N), and oxygen (O) (15). The flexural strength and fatigue strength of CP-Ti increases with a greater amount of oxygen. At room temperature titanium consists of a hexagonal-close-packed cubic structure called alpha phase (α -phase). Above 882°C, the material undergoes an allotropic transformation and will consist of a stronger and more ductile body-centered-cubic crystal structure called beta phase (β -phase). To stabilize the α -, and β -phase, Ti is alloyed with other metals such as aluminum (Al), niobium (Nb) and vanadium (V) (16). Different alloys can thus be designed, α alloys, $\alpha+\beta$ alloys and β alloys. In dentistry, CP-Ti grade 2 and 4 and $\alpha+\beta$ alloys, namely grade 5 (TiAl6V4) and grade 23 (TiAl6V4 ELI-extra low interstitial) are most common (17). The TiAl6V4 ELI alloy has slightly lower amounts of H, Fe and O compared to TiAl6V4. The lower levels of the interstitial atoms, oxygen, hydrogen and nitrogen which are interstitially dissolved in the metal lattice, results in a slightly improved ductility (18). The ultimate tensile strength (UTS) of Ti grade 2 is 345 MPa as compared to 550 MPa for titanium grade 4, and for the $\alpha+\beta$ alloys grade 5 and 23, the strength is between 860–965 MPa. The Young's modulus for all four materials is between 102–114 GPa (17, 19).

1.2 Biocompatibility

Due to the environment of the oral cavity, dental materials must meet certain criteria to be used in patients. Biocompatibility has been described as “the capability of a material to exist in contact with tissues of the human body without causing an unacceptable degree of harm to that body” in a broad sense, or as a material that “shall do no harm to those tissues, achieved through chemical and biological inertness” in a more narrow sense (20).

1.2.1 Cobalt-chromium

CoCr alloys have been used as an alternative to noble alloys in fixed prosthodontics (21), however, there are no randomized controlled studies and there are only a few studies on clinical performance (21-24). No adverse reactions to the material were reported in those clinical studies. Several in vitro and in vivo studies have reported that Ni, Co and Cr are released from dental base metal alloys (25-29). Although, there is no evidence suggesting that metallic dental restorations increase the mutagenic or carcinogenic risk in humans (25), the long-term consequences of the ion leakage are incompletely described both in vitro and in vivo (3, 25, 30, 31). The biocompatibility of CoCr has been investigated in several studies, although mainly in vitro. In one study, the cytotoxicity of different CoCr, NiCr, and

high noble alloys were investigated, and it was concluded that the high noble alloy was significantly less cytotoxic compared to the NiCr and CoCr alloys. Furthermore, there were no significant differences in cytotoxicity between the CoCr and NiCr alloys with comparable amounts of Cr and Mo (32). Stenberg measured the release of Co from removable partial dentures in ten patients using flameless atomic absorption spectrophotometry. The results demonstrated that the released amounts of Co were the highest during the first two days after insertion. However, according to Stenberg, the amount of Co released from the alloy was unlikely to make an obvious contribution to the total Co intake in humans (29). The dental technician handling CoCr alloys in the laboratory may also be exposed to the sensitizing metals in the alloy during grinding or handling metal tools (33, 34). Also, it has been reported that insufficient exhaust ventilation increases the risk of pneumocosis in dental technicians working with CoCrMo alloys (35, 36). In summary, the passive chrome oxide film that spontaneously forms on the surface of the alloy increases the corrosion resistance. Therefore, CoCr alloys are, according to several studies, considered suitable for dental use (27, 37-39).

1.2.2 Titanium

Titanium forms a Ti oxide layer (TiO_2) in contact with oxygen, approximately 5–10 nm thick, which gives the material excellent corrosion resistance (40, 41). Also, this oxide layer is crucial for Ti to be used as an implant material. Titanium has been used as a material for osseointegrated implants since 1965, and several long-term clinical studies with favorable results have been published (42-46). In an in vitro study, the corrosion of cast and CAD/CAM spark eroded CP-Ti grade 1 was tested in a static immersion test. No corrosion was detected and the amount of ion leakage was similar as for Au alloys (47). The corrosion resistance of $\alpha+\beta$ alloys is similar to CP-Ti. However, there has been some concerns regarding slow release of Al and V, since V is considered toxic and Al has been linked to neurological disorders (16). The corrosion behavior of CP-Ti and a TiAl6V4 alloy was analyzed using electrochemical polarization in 37°C Ringer's solution. Both materials showed acceptable resistance to electrochemical corrosion and no ion leakage was detected. However, TiAl6V4 exhibited a higher corrosion rate, which may affect the initial oxide layer stability (48). The cytotoxicity of pure metals and Ti alloyed with different elements was investigated using WST-1 and agar overlay tests. Of the pure metals, CP-Ti grade 2 was the least cytotoxic and in the agar overlay test pure Mn, V, Ag and Cu were moderately cytotoxic. All the Ti alloys, except Ti-10V, were non-cytotoxic. The Ti-10V alloy showed mild cytotoxicity (49). In studies on clinical

performance of Ti dental restorations, no adverse reactions to the material have been reported (50-53).

1.3 Ceramic bond strength

For an alloy to be used in a MC restoration, it must have the ability to create an adherent oxide layer and also have a compatible CTE with the ceramic material (2, 54-56). The thickness of the oxide layer may influence the shear bond strength. However, in a study evaluating the shear bond strength of a ceramic veneering material and a Au alloy, the oxide thickness did not influence the shear bond strength (57). The retention of ceramics to metal restorations is influenced by mechanical forces and chemical bonding as well as van der Waal's forces (58, 59). It is also important that the surface of the metal is not contaminated, and air particle abrasion has been found to increase the shear bond strength of ceramic veneering materials and CoCr (60, 61). Sandblasting of an alloy results in volume loss of the surface, which leads to an increase in surface roughness and wettability (62). According to ISO 9693 (63), a bond between a metal and a veneering ceramic material, evaluated using the Schwickerath crack initiation test, is considered adequate when the bond strength is above 25 MPa.

1.3.1 Cobalt-chromium

Traditionally, CoCr has been used as a material for removable prosthetics but the use of CoCr as an alloy in MC dental restorations has increased in the last decades (64). Compared to noble alloys, CoCr alloys may be more sensitive to laboratory procedures (65). Increased oxidation may result in poor bond strength between metal and veneering ceramic because of chromium ion diffusion, where chromium ions leave the lattice vacancies at the oxide-metal interface resulting in an adhesion fracture between oxide and metal (66, 67). However, the use of a bonder may improve bond strength, by preventing oxide diffusion and neutralizing differences in CTE (66, 68).

The Schwickerath crack initiation test, or three-point bending test, has been used to evaluate the bond strength between CoCr and ceramic veneering materials. Cast CoCr has presented bond strengths above 31 and 46 MPa (10, 69, 70), CNC-milled CoCr above 31 MPa (69), and AM CoCr had a bond strength above 50 MPa (10, 70). The shear bond strength test has also been used to evaluate the bond strength between CoCr and a ceramic veneer. In studies on cast CoCr, the shear bond strength has been above 34 MPa (60, 71-75), and above 60 MPa (76, 77). CNC-milled CoCr had a bond strength above 37 MPa (75), and AM CoCr had bond strengths above 29 as well as 67

MPa (75, 77). In one study, thermocycling significantly lowered the shear bond strengths for cast and CNC-milled CoCr (75). Furthermore, the fracture strength of a veneering ceramic material to CoCr copings manufactured with different techniques, casting, CNC-milling, and additive manufacturing, has been investigated. The results indicated that there were no significant differences between the manufacturing techniques regarding the fracture strength of the ceramic veneering material to the CoCr substructure (78).

1.3.2 Titanium

CP-Ti and Ti-alloys have a high melting point (1668°C) and must be cast in a special casting machine with an argon atmosphere. Also, when the molten metal comes in contact with the investment, a reaction occurs which creates a surface layer called a α -case. The α -case layer, which is rich in oxygen, is hard and brittle and may contain microcracks (79). The α -case layer must be removed using grinding before ceramic veneering (16). Since Ti has a low CTE of about 8–10 and undergoes an allotropic transformation at 882°C, special low-fusing ceramic veneering materials with sintering temperatures below 800°C must be used (16).

The oxide layer that forms on the surface of Ti is important for biocompatibility but also for the bond between Ti and the ceramic veneering material. As mentioned before, the oxide layer that forms in contact with oxygen is only 5–10 nm thick, and will not be significantly affected by oxidation heat treatment up to 750°C. However, if higher temperatures are used, up to 1000°C, the oxide layer will grow to a thickness of one μm . Such a thick oxide layer will significantly decrease the adherence of the oxide to both CP-Ti and TiAl6V4, which will affect the bond strength of the Ti materials and a ceramic veneering material (80).

The bond strength between cast CP-Ti grade 2 and two different veneering ceramic materials with and without a surface modification was studied using the three-point bending test. The mean bond strength values ranged from 17.2 to 24.9 MPa (81). CNC-milled CP-Ti grade 2 had a bond strength above 28 MPa with sandblasting only, and above 35 MPa with a Au sputter coating (82). The bond strength of TiAl6V4 and a ceramic veneering material was above 32 MPa with sandblasting, and was improved further using a borate bonder, up to 49 MPa (83). To increase the bond strength of the ceramic veneering material to Ti a bonder can be applied, good results can be attained using a Au bonder or coatings of Au or Ti nitride (84, 85). A study on the shear bond strength between CP-Ti and different ceramic veneering materials after thermo-, and mechanical cycling showed a decrease in shear bond

strength after treatment. One of the ceramic veneering materials performed better and was closer in bond strength to the AuPd control group than to the other two Ti groups. An explanation to the results may be the use of different bonders for the ceramic veneering within the Ti group (86). A systematic review on the bond between Ti restorations and ceramic veneering materials concluded that the sensitive and reactive nature of Ti requires special handling in the laboratory, with regard to firing temperatures and cleaning of the surface (87).

1.4 Production techniques

1.4.1 Formative manufacturing/Lost wax technique

The traditional technique for production of metal-based dental restorations is the lost wax technique. The technique requires a physical model/cast of the dentition made of type IV stone. For a tooth-supported crown, the stone cast is sectioned to facilitate the die to be removed or lifted from the cast. The preparation line is manually marked or defined using a bur. The abutment is then coated with a hardener and in thin layers using a cement spacer, to create a space between the natural tooth abutment and the inside of the crown. This space will be filled out by the cement at cementation, usually aimed at around 40 μm . The die is thereafter painted with an isolating liquid so the wax crown can be separated from the die. The die is then dipped into a liquid wax that covers the preparation, then the die is placed back into the cast and the crown is built up in wax (88). The finished wax design is sprued and invested in a casting ring with a high temperature investment material. The ring is placed in a furnace to eliminate the wax. The ring is thereafter moved to a casting machine where melted alloy is cast into the mold inside the ring (89). After cooling, the ring is divested and the cast alloy crown is sandblasted using AlO_2 and then cut from the sprue and ground using burs (90).

1.4.2 Subtractive manufacturing/CNC-Milling

When a restoration has been designed using CAD, it can be produced using CAM technology. One technique for manufacturing metal-based dental restorations is CNC-milling, which is a subtractive technique. The CAD-file is transmitted to a software program where the restoration is virtually placed within a selected material block and the milling path decided. The information is used to mill or grind the restoration from a solid block of a material using computer numeric control (91, 92). After milling, the restoration is removed from the material block. A limitation of the technique

is the number of axes, which the milling machine operates with. An increased number of axes makes it possible to mill complex geometries with subsections and convergences (6). Also, the wear of burs and the radius of the milling bur may influence the result, and e.g. limit the milling of the inside of a crown.

1.4.3 Additive manufacturing

Another technique for CAM manufacturing is the additive manufacturing technique (AM). There are several AM techniques available for the production of metals, e.g. direct laser metal sintering (DLMS), selective laser sintering (SLS), selective laser melting (SLM), and electron beam melting (EBM) (91, 93-95). The difference between sintering techniques (DLMS, SLS) and melting techniques (SLM, EBM) is the binding mechanism of the powder particles, where the melting techniques fully melts the powder and creates a more homogenous material (96). The powders used in AM techniques are produced using an atomization process to create a powder with regular size, certain shape and to be free of contaminants (97-99). What the AM techniques have in common, is that the CAD-file is received in a software program, where the restoration is virtually placed on a build platform where build direction and support scaffold is decided and divided into thin layers. A thin coat of a metal powder is spread across a build platform, and a laser or electron beam traces the outline of the first layer, melting the powder particles together. The build platform is lowered and a new coat of metal powder is applied. The next layer is melted and also melted with the layer below it. The laser, or electron beam, traces the outline of the restoration and then fills the interior, for each layer at the corresponding height of the restoration. The process is repeated layer by layer until the restoration is finished (91, 93, 100). Afterwards, the restoration is cut from the build platform and the support scaffolds are removed using pliers. Depending on system and size of the restoration, an annealing process is performed after build in a separate furnace (101). One advantage with the AM technique is the geometrical freedom which allows for fabrication of complex open-cellular structures that can not be achieved using formative or subtractive techniques (94).

1.5 Accuracy and precision

Several studies report the accuracy and precision of manufacturing techniques and restorations. It is important to distinguish between the terms, to understand what has been investigated and reported. The accuracy of a manufacturing technique is the closeness of the produced physical object to

the virtual object or a master object. The precision of a manufacturing technique is the closeness of the results of repeated manufacturing. Ender and Mehl defined accuracy as a deviation from the original object and precision as the accuracy of repeated measurements (102). Persson et al. discussed the accuracy and precision of a measuring system, where accuracy can be seen as how well the measured value represents the “truth”, while precision is the repeatability of the system (103). Brunette also defined accuracy and precision for measurements, accuracy refers to how close the average measurement is to the true value, precision “refers to how close repeated measurements of the same quantity are to each other” (104). Precision has also been defined as the ability of a machine tool or manufacturing process to produce a component to close tolerances (105). Hence, accuracy can be seen as a measurement of the fit of a dental restoration, and precision as a measurement of the reliability of a machine or a manufacturing technique. There are several factors that need to be considered when measuring the fit of a dental restoration, the impression system, the software, the manufacturing technique and the fit measurement technique. In order to measure the accuracy of a restoration, the settings for the internal spacer must be provided. Otherwise, the measurements only reflect the total deviation from the master model, however, since no tooth-supported restoration is manufactured with a 0 μm spacer setting, the results does not represent the accuracy.

1.6 Tooth-supported FDPs

1.6.1 Fixed prostheses for prepared teeth

A well-known and traditional technique for restoring teeth or replacing missing teeth is the FDP, which can be used for a single crown as well as a full-arch bridge (21, 106, 107). The dentist shapes the tooth by using burs depending on the form of the remaining tooth substance, and the restoration to be placed on it. The latter settles the amount of tooth substance to be removed and the outline of the marginal ending e.g. chamfer, slice or shoulder preparation (108). MC restorations have been used extensively since the 1960s, where an understructure, or framework, is made in a metal alloy, anatomically designed to support the ceramic material (88). Several different alloys have been, or are, used for MC FDPs, Au-based alloys, Pd-based alloys, CoCr alloys, NiCr alloys and CP-Ti and Ti alloys. Other materials can also be used for FDP restorations, e.g. zirconia, lithium disilicate (109-112).

1.6.2 Techniques to measure fit

The fit of a tooth-supported restoration can be measured using several approaches. The marginal fit of a restoration can be measured as the marginal gap, the vertical marginal discrepancy, the horizontal marginal discrepancy, and the absolute marginal discrepancy (Figure 3 a-c) (113).

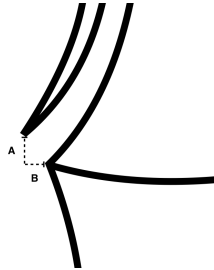


Figure 3 a
A vertical discrepancy
B horizontal discrepancy

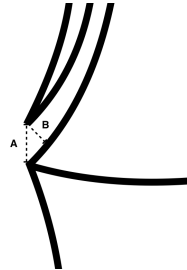


Figure 3 b
A absolute marginal discrepancy
B marginal gap

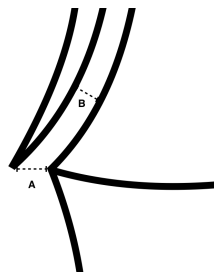


Figure 3 c
A absolute marginal discrepancy
B chamfer/cervical area

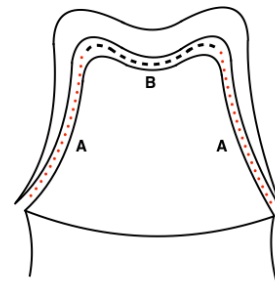


Figure 3 d
A axial discrepancy
B occlusal discrepancy

The internal fit of a restoration, or the cement film thickness, can be divided into discrepancy at the chamfer or cervical area, axial discrepancy and occlusal discrepancy, or as a mean of all the measuring areas/points (Figure 3 c-d) (114, 115). There are different techniques available to measure fit, which can be categorized as either destructive or non-destructive. With the destructive technique, the crown or FDP is cemented onto dies or extracted teeth and then embedded into e.g. epoxy resin, and sectioned. The sections are then analyzed using a microscope (116, 117). The non-destructive techniques are, among others, clinical examination using an explorer, direct view of crown margin on die using a microscope or scanning electron microscopy (SEM) (118, 119), the silicone or impression replica method

(120, 121), micro computer tomography (micro CT) (122) and optical three-dimensional (3D) scanning (123). There are advantages and disadvantages with these methods and the most prominent disadvantage being the restriction to two-dimensional (2D) analyses, but also in suffering from a limited number of measuring points (117). According to a study by Groten, at least 50 measurements per tooth is required to measure the vertical marginal fit of crowns (118). However, several studies base their measurements of the marginal gap on two to eight measurement points per abutment/crown (116, 117, 124, 125). The silicone replica method is a valuable technique for measuring fit in vivo, but there are limitations regarding the technique i.e. the light-body impression material may rupture in the marginal gap area when the restoration is removed and there may be uncertainty regarding the placement and direction of the sections (126). However, Falk et al. evaluated the reliability of the method and found it useful for analyzing marginal and internal fit (121).

1.6.3 Impact of misfit

The fit is an important factor that influences the clinical longevity of a restoration, and both marginal and internal fit has to be considered (113, 117). A gap at the margin of a restoration can affect the cement junction and result in dissolution. This may result in loosening of the restoration and secondary caries (127). An increased marginal gap in subgingivally placed margins may increase bacterial retention and cause gingival inflammation (128). For a proper seating of a crown, an internal gap of at least 40 μm is needed (129, 130). However, an increased internal cement film thickness may decrease the retentive force of the cement and the retention of the dental crown (131). Therefore, the ADA and ISO states the required maximum film thickness to 25 μm for water-based cement and 40 μm for resin-based cement (132, 133). Several factors influence the fit of a restoration, such as the preparation type and taper, the amount of cement used, the pressure during cementation and the viscosity of the cement (134-136).

A mean marginal gap of approximately 100 μm has been regarded as clinically acceptable by several authors (120, 126, 127, 137, 138). McLean and von Fraunhofer considered a marginal and internal gap of 120 μm clinically acceptable for dental restorations cemented with polycarboxylate cement (120, 127). However, over the years, studies on marginal gap have debated on what distance is to be considered as clinically acceptable. In a study by Christensen, the mean opening of gingival margins of gold inlays, not crowns, was regarded as clinically acceptable at 74 μm by experienced dentists using an explorer (139). Some studies cite Jørgensen (136) and

Ishikiriama (135), however, their studies analyze factors affecting the cement film thickness, not what is clinically acceptable. Hence, what is clinically acceptable is not clearly defined. In a study by Bronson et al. (140), the clinical acceptability of marginal gaps, as determined by pre-doctoral students and prosthodontists was evaluated. The marginal gaps ranged from 40 to 615 μm . Both students and prosthodontists rated marginal gaps up to 200 μm as clinically acceptable. According to Ryge (141-143), rating scales for clinical examinations of restorative materials may be used. Where the *Alfa* rating should be given if the explorer does not “catch” when drawn over the restoration-tooth margin. If the explorer “catches” at the margin, the *Bravo* rating should be given. The *Charlie* rating is given when the explorer penetrates the gap and the dentin is exposed. McLean and von Fraunhofer discussed the diameter of the explorer tip, and an explorer with a 50 μm tip was measured after three weeks of use. The results demonstrated that the tip had been blunted due to plastic deformation. Hence, a 50 μm explorer tip could fail to “catch” an 80 μm margin gap after a few weeks of use (120). In a study by Hickel et al., recommendations for clinical studies of restorative materials/inlays were presented. Explorers with different tip diameters (50, 150 and 250 μm) should be used to measure marginal gaps. If a 250 μm explorer tip “catches” a gap, the restoration should be regarded as clinically unacceptable (144). In yet another study, experienced dentists evaluated non-visible margins using an explorer. Their ratings for acceptable openings ranged from 32–230 μm for the horizontally open margins and 43–196 μm for the vertically open margins (145). Although the internal fit and cement film thickness of dental restorations is important for the retention (146), it has not been studied to the same extent as the marginal fit.

1.6.4 Fit of tooth-supported CoCr FDPs

CNC-milled CoCr four-unit FDPs with a spacer setting of 30 μm , measured with the silicone replica technique, have demonstrated marginal gaps of 56.9 and 90.64 μm (147). Three-unit FDPs with a spacer setting of 25 μm , evaluated with the silicone replica technique, have shown an absolute marginal discrepancy of 94.29 μm (148), and in another study, with a spacer setting of 50 μm , the absolute marginal discrepancy was 225.5 μm . The FDPs were cemented, embedded in epoxy and sectioned mesiodistally in one plane (117). For the same restorations, the discrepancy in the chamfer area was 67.01 μm and 108.85 μm with a 30 μm spacer, and 47.97 μm for the 25 μm spacer (147, 148). The internal discrepancy was 96.77 μm for the 25 μm spacer and 166 μm for the 50 μm spacer (117, 148). The occlusal discrepancy was 278 μm for the 50 μm spacer, and 198.1 μm and 215.71 μm for the 60 μm spacer (117, 147).

Studies on CoCr single crowns fabricated with the AM technique have demonstrated mean marginal gaps between 93 μm and 102.86 μm , and an occlusal mean discrepancy of 252 μm , using the silicone replica technique (149, 150). The mean chamfer area discrepancy was 76 μm . Ucar and colleagues evaluated the fit of AM CoCr crowns by embedding and sectioning the crowns labio-lingually. A mean internal discrepancy (occlusal and axial) of 62.6 μm (151) was reported. The fit of three-unit FDPs with different spacer settings fabricated using the AM technique, and analyzed using the silicone replica technique, has been evaluated by different research groups. The mean absolute marginal discrepancy was 89.5 μm for the 50 μm spacer and 130.5 μm for the 30 μm setting, and a mean internal discrepancy of 84 μm for the 50 μm spacer and 188.32 μm for the 25 μm (117, 148, 152). Also, the marginal gap was studied, FDPs with the 25 μm spacer setting had 70.98 μm and FDPs with the 30 μm spacer had a marginal gap of 112.65 μm (152).

Most authors conclude that the results from their in vitro fit studies are within the limits of clinical acceptability, regardless of material investigated, when the mean marginal gap is below or close to 120 μm . Even though, the internal discrepancies in these studies may be well over 200–300 μm (147, 149, 153-155). However, in one study using the silicone replica technique, the internal fit of AM CoCr crowns a mean occlusal discrepancy over 250 μm was shown. The authors regarded the fit as clinically unacceptable (156).

1.7 Implant-supported FDPs

1.7.1 Prostheses for osseointegrated implants

Since Brånemark's discovery in the early 1960s, that Ti implants are tolerated by the tissues, and that the bone can form close to the Ti surface, prostheses could also be anchored to implants (42). The ankylotic character of the dental implant requires a higher level of fit to avoid biological and technical complications (157, 158). Initially, frameworks for implant-supported bridges were cast in sections and soldered, or in one-piece castings, using the lost-wax technique. The material used was a Au alloy with acrylic, or occasionally ceramic, veneering. However, the ceramic layer was usually placed as a buccal or facial veneer only and the occlusal surface was in Au. The large bulk of Au material caused misfit of FDPs resulting in fixture fractures (45). To overcome this problem, a less bulky Au structure was used, with acrylic or composite resin teeth on the occlusal surfaces (159). The process of investing the wax-up and casting implant frameworks is complicated and technique-sensitive, usually resulting in misfit (160-162).

To overcome this problem, frameworks have been sectioned and soldered or laser-welded vertically and horizontally. Horizontally sectioned and laser-welded frameworks in Ti and CoCr using the Cresco™ method have worked well in clinical situations (163, 164). According to Riedy and colleagues, laser-welded frameworks in Ti had better fit compared to one-piece cast frameworks (165). Early attempts to industrialize the manufacturing of implant frameworks included prefabricated framework sections that were laser-welded together in order to fit a specific patient. However, laser-welded frameworks had more fractures and complications compared to cast Au alloy frameworks after 15 years (166). In the late 1990s Ti-frameworks fabricated using CNC-milling machines were introduced. According to several studies, CNC-milled Ti frameworks have a better fit compared to cast frameworks made from different alloys, frameworks produced using the Cresco™ method, and CNC-milled zirconia (167-172). There has been a rapid development of digital technologies in dentistry (173) and according to a consensus statement, CAD/CAM technologies have been successfully implemented into implant dentistry (174).

1.7.2 Techniques to measure fit of implant-supported FDPs

There are several techniques available to measure the fit of implant-supported prostheses. Clinically, the dentist can detect a misfit when tightening the bridge screws or if a gap between framework and abutment/implant is detectable with a sharp explorer (175). The one-screw fit test, radiographs, the silicone replica technique and photogrammetry can also be used to measure the fit in vivo (158, 176-178). In vitro techniques for fit measurements include, among others, the strain-gauge test, coordinate measuring machine (CMM), optical microscope, photogrammetry, SEM, laser videography (165, 169, 179, 180). In the strain-gauge test, the stress on the implant components from the framework structure can be measured. However, the strain measurements are limited to the area where the strain gauges are attached (160, 181). Scanning electron microscopy and other microscopes can be used to measure the vertical gap distance between framework and abutment, it requires standardization and is limited to a 2D analysis (170, 182-184). The photogrammetry, laser videography and CMM techniques are all able to record data in three dimensions and register the center point or centroid of the abutments and framework implant connections. The center points from the framework are “superimposed” onto the abutment center points and any discrepancy between two center points is measured in the x-, and y-axes as well as the z-axis (185-187). The alignment of the center points can be done using the method of least squares or “best

fit” method, as well as the “zero“-, or “orthogonal 3-2-1” method (172, 188). With the “best fit” method the center points from the framework are placed in the theoretically best position to the abutments on the model. With the “zero” method and five implants, one of the implants is chosen as the zero position for the x-, y-, and z-axes, the third implant is used for alignment in the z-axis and the fifth implant is aligned in the x-, and y-axes. Both the “best fit”-, and the “zero” methods employ a theoretical placement of the framework, resulting in a “virtual” fit of the framework, underestimating the vertical distortion (172, 189, 190).

1.7.3 Fit of implant-supported FDPs

Several authors have attempted to define “passive” fit with the acceptance of a certain degree of vertical misfit, ranging from 40–150 μm (157, 158), although there is yet no consensus. Others have tried to define “passive” fit as “fit which is less than perfect, but the application of any external forces to produce a perfect fit has a negligible effect on the performance of the prosthesis” (191), or as “to provide passive fit or a strain-free superstructure, a framework should, theoretically, induce absolute zero strain on the supporting implant components and the surrounding bone in the absence of an applied external load” (192). Although perfect accuracy is only achievable in theory (19), the limits for clinical acceptance are still disputed. It has been described that framework strain can be affected by the vertical misfit (193, 194), and a misfit between framework and abutment increases the external preload. The internal preload is the tension between the abutment and the prosthesis after the screws are tightened. The external preload is the static axial force between the implant and framework due to misfit (195).

1.7.4 Impact of misfit

The importance of passive fit relating to biological and technical complications is still debated and so far no study has produced frameworks with a passive fit (189). Contradicting results have been reported concerning the impact of misfit on the surrounding bone. In a study using FEA, the stress distribution in the surrounding bone was analyzed for implant-supported prostheses with 0 or 111 μm misfit. A misfit resulted in higher levels of stress in the surrounding bone, and the presence of a cantilever or increased occlusal force amplified the effect (196). In one experimental animal study it was demonstrated that the surrounding bone was negatively affected, with greater bone loss (density), by implants under dynamic load (197). However, other animal studies have shown that prostheses with misfit did not lead to biologic failure, but may instead promote bone remodeling (198-200). In a clinical study following seven patients prospectively for one year and seven

patients retrospectively after five years, comparing cast Au and acrylic veneered fixed prostheses with different levels of misfit placed on five to seven implants. The mean misfit regarding center point positions was 111 (SD 59) μm for the one year group and 91 (SD 51) μm for the five year group, no differences in marginal bone loss were reported (201). When considering technical failures, veneer fracture is the most common complication, followed by screw loosening and screw fracture, according to two systematic reviews (202, 203). Framework misfit could be an important factor regarding technical complications, since the greatest stress in a prosthesis with misfit is focused on the bridge screw (196).

1.8 Ceramic veneering of FDPs

For esthetic reasons, the visible parts of a crown or a FDP are most often covered with a ceramic layer. The veneering process of a metal substructure or framework includes several manual steps. Each ceramic layer is built up by hand and thereafter sintered in a furnace. The manufacturing of a crown usually requires approximately six to seven firings, at temperatures ranging from 870°C to 980°C.

The ceramic veneering process may influence the fit of MC prostheses (108, 137, 204-209). In a study by Sundar et al. evaluating the fit using a microscope with 40x magnification, the mean marginal gap of cast CoCr crowns increased from 66.2 μm to 70.8 μm , and for AM CoCr crowns the marginal gap decreased from 56.3 μm to 53.6 μm after veneering (119). Richter-Snapp et al. also used the direct view microscope technique, with a magnification of 40x, and found changes in fit during the different stages of firing, but no significant effect on the final marginal fit of crowns was described (210). Moreover, in another study the oxidation heat treatment cycle was found to cause the most horizontal distortion in three-unit cast Pd alloy implant frameworks, using the direct view technique with a magnification of 200x (211). Similar results were found in a study by Gemalmaz et al. where the horizontal distortion was the largest after the oxidation cycle for cast three-unit FDPs in NiCr and PdCu. The vertical distortion was the highest after the glaze cycle. In that study the fit was measured using the silicone replica technique and by measuring the length and vertical height using a digital micrometer (212). The distortion after the first heat treatment may be attributed to stress within the metal framework resulting from casting and cold working during the manufacturing process (213-215). Long-span FDPs following the curvature of the jaw have been found to contract in the posterior dimension and move labially in the anterior

dimension, possibly due to the contracting effect of the ceramic material (215). However, Anusavice and Carroll analyzed the effect of incompatibility stress, mismatch in CTE ($+2.2 \times 10^{-6}/^{\circ}\text{C}$), on the fit of MC crowns. They disregarded the mismatch in CTE as a cause of distortion since there was no difference in mean gap compared to crowns veneered with compatible ceramic, and suggested external grinding and internal abrasive blasting as more likely causes (216).

In contrast, studies have shown that the fit is not affected by the veneering process since castings of a AuPd alloy were not affected by heat treatment when evaluated using the direct view technique using a microscope with a magnification of 100x (217). The marginal fit of machine-milled and spark-eroded Ti crowns were evaluated by using a travelling microscope with a magnification of 100x. The fit of the crowns was not significantly affected by ceramic veneering (125). In two other studies the fit before and after simulated ceramic firings was not significantly affected. This was described for both full-arch implant-supported Ti frameworks evaluated using a CMM, but also for cast three-unit CoCr and Ti frameworks evaluated using the one-screw fit test (169, 218).

In one study, the opaque layer firing temperature and aging effect on the flexural bond strength of a ceramic veneering material to a cast CoCr alloy were evaluated (219). It was concluded that an increased firing temperature increased the flexural bond strength between the ceramic veneering material and CoCr.

Clinical follow-up studies on CoCr restorations are scarce, however, in one study 51 CoCr FDPs in patients with severely compromised dentition was followed for three to seven years. Seventeen of the FDPs had biological and/or technical problems i.e. loss of retention, framework fracture, root fracture, and endodontic and periodontal complications. Furthermore, nine FDPs had ceramic fractures, one major and eight minor fractures (21). In yet another clinical study (mean observation time 47 months) AM CoCr and AM AuPt MC crowns were evaluated. There were no significant differences in failures between the two materials, and interestingly, no ceramic chipping was reported (23). In a five-year follow-up study on 15 ceramic veneered CoCr implant prostheses in the maxilla, no significant differences were shown compared to 25 Ti counterparts veneered with acrylic teeth. However, four out of 15 prostheses had ceramic fractures (22).

Regarding Ti restorations, a high rate of ceramic chip off fractures has been reported in clinical follow-up studies. Kaus et al. followed 84 restorations

with 125 veneers for three years. Ceramic fractures were reported for 25.9% of the veneers and mainly in the multi-unit FDPs (53). In another study of 41 single crowns, followed for six years, ceramic fractures in 27% of the crowns were reported. The high fracture rate may be explained by a uniform thickness of the copings and thus an insufficient support for the veneering ceramic material (220). In contrast, Milleding et al. followed 40 single crowns for two years with only one ceramic fracture (221), and Nilson et al. reported two fractures in 44 crowns after 26–30 months (222).

2 BACKGROUND TO THE PRESENT THESIS

Even though there are only a few clinical studies published on the performance of cobalt-chromium restorations, it is extensively used as a material in fixed prosthodontics. Thus, there is a need of long-term follow-up studies of CoCr restorations. Moreover, the manufacturing process of CoCr has changed in the last five years, from the formative lost wax technique to subtractive CNC-milling, and to additive manufacturing. The CAD/CAM techniques have already been implemented in the dental laboratories, but using a digital workflow from clinic to laboratory involves intraoral digital impressions in the clinic. There are some studies on the fit of single crowns manufactured using digital impressions, the effect of the digital impressions on the fit of multi-unit FDPs need to be evaluated.

Studies have shown that CNC-milled Ti frameworks for implant-supported FDPs are superior to cast FDPs. Today, other materials and techniques have been introduced and need to be compared to CNC-milled Ti frameworks. CoCr alloys are now CNC-milled and also manufactured using additive manufacturing. Ti frameworks can also be additively manufactured. The fit of these frameworks need to be evaluated.

CoCr FDPs are not usually made as full-contour or full-anatomic restorations. They are instead designed using a cutback technique and then covered with a ceramic surface for a tooth-like appearance. Both the CoCr and Ti frameworks are veneered with ceramics for esthetic reasons, the process of veneering a metal framework with ceramics subjects the framework to repeated heat treatments, which could affect the fit of the FDP. It is of great interest to evaluate the effect of ceramic veneering for FDPs of both CoCr and Ti that have been manufactured using these new techniques.

2.1 Design of the thesis

The thesis is comprised of three parts, part one is a clinical study of tooth-supported CoCr FDPs, part two evaluates the effect of the digital impression on the fit of tooth-supported CoCr FDPs and part three is based on the fit of implant-supported FDPs in CoCr and Ti and the effect of ceramic veneering.

Part 1. Clinical study on tooth-supported CoCr FDPs (I).

Part 1 is a retrospective clinical five-year follow-up study on tooth-supported CoCr FDPs manufactured using the formative lost wax technique.

Part 2. In vitro study on digital and conventional impressions for tooth-supported FDPs (II).

Part 2 is an in vitro study on the fit of tooth-supported CNC-milled three-unit CoCr FDPs generated from digital and conventional VPS impressions.

Part 3. In vitro studies on the fit of CNC-milled and additively manufactured CoCr and Ti frameworks for implant-supported FDPs, and the effect of ceramic veneering (III-IV).

Part 3 is comprised of two studies evaluating the fit of CoCr and Ti implant-supported frameworks manufactured using subtractive CNC-milling and additive manufacturing. Also, the effect of ceramic veneering on the fit is evaluated.

2.2 Aim

The overall aim of this thesis was to study CAD/CAM production processes, material aspects on cobalt-chromium and clinical survival/success, and fit of tooth-, and implant-supported fixed dental prostheses.

2.3 Specific aims

The specific aims of the studies in this thesis were:

- Paper I: To evaluate the five-year clinical outcome of ceramic veneered CoCr FDPs inserted in a private clinical setting.
- Paper II: To evaluate the marginal and internal fit of CNC-milled CoCr three-unit FDPs produced from digital and conventional VPS impressions using a triple-scan protocol for 3D fit assessment.
- Paper III: To evaluate the fit of CNC-milled CoCr and Ti implant-supported frameworks in an edentulous maxilla, provided with six implants.

To evaluate the effect of ceramic veneering on the fit of the CoCr frameworks.

Paper IV: To evaluate the fit of CNC-milled Ti, additively manufactured CoCr and Ti implant-supported frameworks before and after ceramic veneering.

2.4 Hypotheses

Paper I: That CoCr FDPs function well in a clinical situation during a follow-up period of five years.

Paper II: That there is no difference in fit of FDPs produced from digital and conventional VPS impression techniques. The alternative hypothesis is that there is a difference in fit of the FDPs, the direction of the difference is yet unknown.

Paper III: That the fit of CNC-milled CoCr frameworks is similar to the fit of Ti frameworks.

That the fit of CNC-milled CoCr FDPs is unaffected by ceramic veneering.

Paper IV: That the fit of additively manufactured CoCr and Ti frameworks are similar to CNC-milled frameworks.

That there is a difference in fit before and after ceramic veneering.

3 MATERIAL AND METHODS

3.1 Part 1. Clinical study on tooth-supported CoCr FDPs (I).

3.1.1 Retrospective clinical study (I)

The clinical study was a five-year retrospective evaluation of dental records of patients treated with multi-unit CoCr FDPs. The treatments were performed in a private clinical setting in Sweden by two experienced clinicians (two of the authors). The impressions were made with hydrocolloid-alginate impression material (Image, Dux B.V; Blueprint cremix, Dentsply). The FDPs were manufactured at one dental laboratory using the lost wax technique and a CoCr alloy (Wirobond C, BEGO). CoCr was the only MC material used at the clinic in question at the time of the study (since 1999). The ceramic veneering of the frameworks was done using ceramic bonder (Ceram-Bond, Bredent) and feldspar ceramics, Noritake (Noritake EX-3) or Duceram Plus (Duceram Plus, Degudent) depending on the technician. Most FDPs (191) were cemented with zinc phosphate cement (Harvard cement, Harvard Dental International) and eleven FDPs were cemented with Rely X (Rely X Unicem, 3M ESPE).

3.1.2 Follow-up, dental records and radiographic examination

Patients were given hygiene information by a dental hygienist after cementation and were scheduled for follow-up at least once a year. There were no extra recalls for clinical examinations. The patients were examined and data recorded by the clinician who performed the treatment during the follow-up period, and the records were reviewed later (September 2010 to February 2011).

A number of factors such as age, sex, number of units, radiologic status, type of cement, and occluding teeth in the opposing arch were recorded. Furthermore, all complications that may have occurred were registered. Complications were biologic (caries, gingivitis/mucosal, periodontal problems, root fillings, root fractures) and technical (cohesive ceramic fractures, cementation failure).

3.1.3 Patients

One hundred forty-nine consecutive patients received 201 CoCr FDPs from January 2000 to November 2005. Of the patient group, 52.3% were women and the mean age at the time of cementation was 66.8 years (range: 39 to 90 years).

The 201 FDPs consisted of 1,135 units (mean: 5.7 per FDP; range: 2 to 14), 743 abutments (mean: 3.7 per FDP; range: 1 to 9), and 392 pontics (mean: 1.95 per FDP; range: 1 to 6). The pontic/abutment ratio was 0.53. Of 392 pontics, 112 were cantilever pontics in 79 FDPs. Of the 112 cantilever pontics, 56 were unilateral and 56 were bilateral. Four were mesial pontics and 108 were distal. The mean pontic/abutment ratio for the cantilever FDPs was 0.57. One hundred thirty-seven FDPs were short-span FDPs (two to five units) and 64 were long-span (six or more units).

Of the 743 abutment teeth, 221 were root filled at cementation. One hundred twenty-eight teeth had an indirect post (127 gold alloy and one titanium), 23 had screw posts, 17 had composite posts, and the remaining 53 were left with no post. In the opposite arch, most patients had teeth or fixed prostheses. Only four patients had removable dental prostheses.

3.1.4 Definitions

Success was defined as the reconstruction remaining unchanged without requiring any intervention during the observation period. With this definition, any complication during the follow-up period resulted in a failure classification.

Survival was defined as the reconstruction remaining in situ after five years, with or without modifications, as per Tan et al. (223).

However, if the FDP was shortened or reduced to a single crown, if the FDP was remade due to cement failure or veneer fracture, or if the abutment teeth were extracted, it was considered a failure. If a patient lost an FDP and received a new FDP during the follow-up period, the new FDP was not included. The longevity of the FDPs was counted from cementation to the year of the first complication that led to a failure classification within the definition of success, and subsequently for the definition of survival.

The results can also be defined in actual outcomes, i.e. the state of the patient cohort in year five. To better describe the results and make them more comparable with other studies, Walton's definitions of outcomes (106) was

also applied to the material.

These definitions are briefly described as follows:

- *Successful*: no evidence of retreatment other than maintenance procedures, including minor occlusal adjustments, without compromising the esthetics
- *Surviving*: third party examination or confirmation of no retreatment other than for successful outcome
- *Unknown*: patient could not be traced; surviving or successful prosthesis removed to allow for a new prosthesis
- *Retreatment (repair)*: original marginal integrity of the retainers and teeth is maintained (endodontic therapy through retainer not considered repair)
- *Retreatment (failed)*: part or all of retainer has been lost, modification to the marginal integrity, or a retainer has been recemented more than twice after cementation

3.1.5 Statistical analysis

The cumulative success/survival rates (CSRs) were calculated according to actuarial life table techniques, and standard errors were calculated using the Greenwood formula (224). The CSR values presented represent events occurring from cementation day to year five.

3.2 Part 2. In vitro study on digital and conventional VPS impressions for tooth-supported FDPs (II).

3.2.1 Study casts

To standardize the study casts, the master cast was duplicated using four silicone molds (Zhermack duplication silicone, elite double 32 extra fast, Zhermack SpA, Badia Polesine, Italy). The molds were cast with type IV stone (Shera Hard Rock, Shera Werkstoff Technologie GmbH & Co, Lenförde, Germany) to achieve 20 casts. The 20 study casts were assigned by blind randomization to control and test groups, with ten casts in each group (Figure 4).

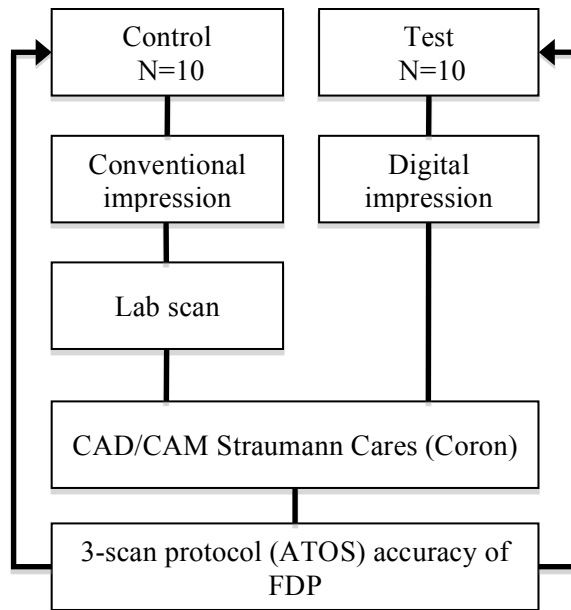


Figure 4. Study design paper II.

3.2.2 Conventional VPS impressions (control group)

The conventional impression technique was performed by one of the authors using individually designed impression trays (Photo-Tray, light-curing baseplates, Dentalfarm, Torino, Italy). An adhesive for vinyl polysiloxane (VPS) impression material (VPS Tray Adhesive, 3M ESPE, Seefeld, Germany) was applied to the trays five to ten minutes before impression. Putty-wash impressions were taken using VPS material (Honigum light body and heavy body impression material, Honigum®, DMG, Hamburg, Germany). Impressions were set under finger pressure for five minutes at room temperature. One experienced prosthodontist and one experienced dental technician examined the impressions for tears and voids and connection between tray and impression material. The impressions were poured with type IV stone (Shera Hard Rock). Conventional laboratory procedures were used to fabricate a working cast with removable sections. The die sections were ground, using conventional burs for stone, for easier access to the preparation lines (Figure 5).

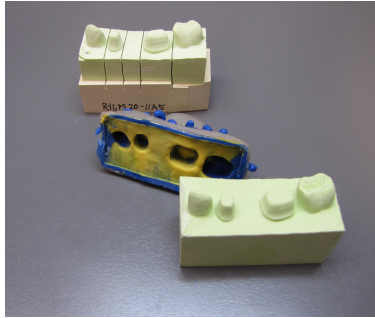


Figure 5. Study cast, conventional VPS impression and working cast with removable sections.

3.2.3 Digital impressions (test group)

An intraoral scanner (Cadent iTero, Tel Aviv, Israel) was used to perform the digital impressions of the ten test casts (Figure 6 & 7). The hand-held scanner uses the confocal light technique to capture images. A series of five scans per abutment were taken, followed by additional scans to record the remainder of the quadrant and antagonist. After an assimilation process, a 3D model of the scanned arch was produced. The scan was controlled and the preparation margin was checked. The file was then sent to a workstation and prepared by one of the authors with reference to preparation margin and insertion path.



Figure 6. Digital impression device.

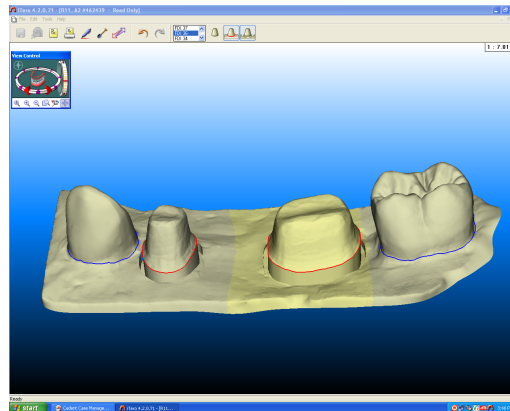


Figure 7. Digital impression of study cast.

3.2.4 Fabrication of three-unit CoCr FDPs

The working casts were scanned using a Straumann Cares 2 scanner and the files were transmitted into the Cares CAD software (CARES VISUAL 6.2). The files from the digital impressions were then downloaded to a Straumann Cares workstation and three-unit FDPs with a cutback design for metal ceramics were designed using Cares CAD software (CARES VISUAL 6.2) (Figure 8). The cement gap (0.5mm closest to the finish line) was set at 30 μm , the spacer gap (beginning above the cement gap) was set at 60 μm , and the correction of milling radius was set at 110% in the cusp areas. The minimum restoration thickness was set at 0.4 mm, the thickness at the finishing line was set at 80 μm , and the cutting angle was 20°. The CAD files were then transmitted to a production facility (Straumann, Leipzig, Germany) where the frameworks were CNC-milled in a CoCr alloy (Coron Co bal %, Cr 28%, W 8.5%, Si 1.65%, Mn < 1%, N < 1%, Nb < 1%, Fe < 1%, Straumann). The marking of finishing lines, approval of intraoral scans, and designing of all FDPs were performed by one of the authors.

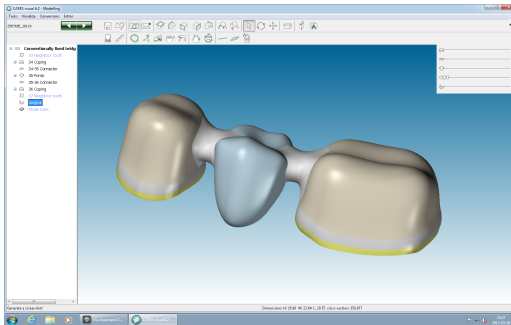


Figure 8. CAD image of designed cutback FDP framework.

All FDPs were tested on their respective study cast upon arrival. One FDP from the control group was considered clinically unacceptable due to misfit; that is, it fitted well to the working cast but not to the study cast. The impression technique and/or working cast production were considered the reason for misfit. The FDP was therefore not used and a new impression was made on the study cast. From the new impression, a working cast was made and a new FDP was fabricated and scanned according to the established protocol. The frameworks were not adapted for a better fit but measured in the as-delivered state.

3.2.5 Analysis of fit

A noncontact ATOS III triple-scan (GOM, mbH, Braunschweig, Germany)

scanner with blue-light technology was used to determine the fit of the FDPs to the study casts, using triangulation. The scanning was performed according to the triple-scan protocol for 3D fit assessment used by Holst et al. (123). According to Holst et al., the repeatability of the technique was almost perfect, revealing an intra class correlation coefficient of $r = 0.981$. First the cast and the inside of the restoration were scanned separately, then a positioning scan with the restoration placed on the cast was performed. The distances from the abutment surface to the inside of the FDP were measured from 250,000 to 400,000 points per abutment resulting in a point cloud representing the discrepancy between the two surfaces. Experienced operators performed the scanning procedure. The scanning information was then put together in CAD software (GOM Inspect v7.5, GOM mbH, Braunschweig, Germany), and the discrepancy between each abutment and the corresponding inner surface of the retainer was calculated for the FDP. The internal discrepancy was calculated as a mean of all distances between abutment and inner surface of the retainer. The absolute marginal discrepancy was measured from the finish line to the crown margin circumferential and a mean was obtained using the CAD software, and hence this measurement includes both marginal gap and under- or overextension of the crown. The cervical area discrepancy was measured from the 0.5mm closest to the finish line circumference. All analyses of discrepancies were performed by two of the authors. The settings for distance measurements were maximum distance 0.4 mm, maximum deviation of normals 60° , and maximum opening angle 30° .

3.2.6 Statistical analysis

The fit of the FDPs was compared in terms of the impression method in three ways: mean internal discrepancy, absolute marginal discrepancy, and cervical area discrepancy. The Mann-Whitney U test was used to detect significant differences between the test and the control group. The distribution was confirmed using box plots. The significance level was set at $P < 0.01$.

3.3 Part 3. In vitro studies on the fit of CNC-milled and additively manufactured CoCr and Ti frameworks for implant-supported FDPs, and the effect of ceramic veneering (III-IV).

3.3.1 Fabrication of master models and acrylic resin pattern

A model of an edentulous maxilla in type IV stone was fitted with six implant abutment replicas (Ankylos, Balance Base Abutment narrow 5.5, Dentsply, Sirona Implants, Mannheim, Germany) and duplicated ten times using duplicating silicone (Zhermack Duplication Silicone, Elite Double 32 Extra Fast, Zhermack SpA, Badia Polesine, Italy), type IV stone (Shera Hard Rock, Shera Werkstoff Technologie GmbH & Co, Lenförde, Germany) and Ankylos Balance Base retention copings. One acrylic resin pattern simulating a patient case (designed for ceramic veneering) was made from a tooth-setup and used for fabrication of frameworks on abutment level. The ten models and the acrylic resin pattern were sent to a production center (Atlantis suprastructures, Dentsply Sirona Implants, Hasselt, Belgium) where they were scanned and the files prepared using CAD software.

Table 1. Cobalt-chromium alloy composition in percent (weight %)

Material	Co	Cr	Mo	W	Fe	Si	Mn	Nb
CNC CoCr*	54.1	20.0	-	16.4	7.5	1.5	0.3	0.2
AM CoCr [§]	63.9	24.7	5.0	5.4	-	<1	-	-

*Starloy Soft (Dentsply-DeguDent)

[§] Renishaw Laser PFM DG1 (Renishaw)

3.3.2 Fabrication of CoCr frameworks

Ten frameworks were CNC-milled in CoCr (Starloy Soft, Dentsply, DeguDent, Hanau-Wolfgang, Germany), one for each model (Table 1). According to the manufacturer, the horizontal tolerance of the milling procedure was five µm. Also, ten frameworks, one for each model, were additively manufactured in a Renishaw AM 250, with Renishaw DG1 powder (Renishaw, Wotton-under-Edge, Gloucestershire, United Kingdom) using 40µm layer thickness. After build, the frameworks were stress relieved using a heat treatment process in a furnace with argon atmosphere. The implant mating surfaces were thereafter milled using a five-axis CNC-milling

machine (Willemin Macodel, Delémont, Switzerland) (Figure 9).



Figure 9. AM CoCr framework before ceramic veneering.

Table 2. Titanium and titanium alloy composition in percent (weight %)

Material	Ti	Al	V	Fe	O	H	C	N
CNC Ti*	Bal	-	-	>.50	>.40	>.10	>.10	>.05
AM Ti [§]	Bal	6.45	4.0	0.23	0.12	0.0052	0.01	0.01

*Grade 4

[§]Grade 23

3.3.3 Fabrication of Ti frameworks

Ten frameworks were CNC-milled in Ti (CP grade 4), one for each model. According to the manufacturer, the horizontal tolerance of the milling procedure was five µm. Also, ten frameworks were additively manufactured using a Renishaw AM 250, with TiAl6V4 extra low interstitial (ELI) powder for the Ti frameworks, (Table 2) (Renishaw, Wotton-under-Edge, Gloucestershire, United Kingdom) using 40µm layer thickness. After build, the frameworks were stress relieved using a heat treatment process in furnace with argon atmosphere. The implant mating surfaces were thereafter milled using a five-axis CNC-milling machine (Willemin Macodel, Delémont, Switzerland).

3.3.4 Ceramic veneering of frameworks

The ceramic veneering of the frameworks was performed at a commercial dental laboratory by experienced dental technicians. The veneering procedure for the CoCr frameworks, furnace and firing cycles are described in table 3 (GC Initial MC, GC Nordic AB, Älvsjö, Sweden), and for the Ti frameworks in table 4 (GC Initial Ti, GC Nordic AB, Älvsjö, Sweden). After veneering, the visible metal surfaces were polished and the mating surfaces on the frameworks were blasted with 50 µm glass beads at two to three bar (Magma

50 μm , M-Tec Dental AB, Malmö, Sweden) to remove the oxide that had accumulated during the firing cycles (Figure 10).

Table 3. Ceramic veneering procedure of the CoCr frameworks. Firing cycles and materials. Furnace Ivoclar Programat P90.

n	Program	Material*	End temp
1	Oxidation	N/A	950°C
1	Bonding	GC Initial Metalbond	980°C
1	Opaque 1	GC Initial MC Paste Opaque	960°C
1	Opaque 2	GC Initial MC Paste Opaque	950°C
2	Dentin	GC Initial MC Dentin	905°C
		GC Initial MC Enamel	
1	Glaze	N/A	870°C

n = number of firing cycles

* = GC Initial MC, GC Nordic AB, Älvsjö, Sweden

Table 4. Ceramic veneering procedure of the Ti frameworks. Firing cycles and materials. Furnace Dentsply DeTrey Multimat C.

n	Program	Material*	End temp
1	Bonding	GC Initial Ti Bonder	820°C
1	Opaque 1	GC Initial Ti Powder Opaque	820°C
1	Opaque 2	GC Initial Ti Powder Opaque	820°C
2	Dentin	GC Initial Ti Dentin	820°C
		GC Initial Ti Enamel	815°C
1	Glaze	N/A	795°C

n = number of firing cycles

* = GC Initial Ti, GC Nordic AB, Älvsjö, Sweden



Figure 10. Finished CNC-milled CoCr FDP after ceramic veneering.

3.3.5 Analysis of fit

After fabrication of the frameworks, they were analyzed regarding fit to the corresponding casts. The stone casts and frameworks were sent to an independent measuring laboratory in Sweden (Mylab AB, Gothenburg, Sweden). The mating surfaces of the abutment replicas and frameworks were measured with a CMM (Zeiss Prismo Vast, Carl Zeiss Industrielle Messtechnik GmbH, Oberkochen, Germany). Each stone cast and corresponding Ti and CoCr framework was measured with a scanning head equipped with a contact stylus, which could be positioned at any x-, y-, z-location within the CMM working space. The position and angulation of the center point of all abutment replicas and the corresponding framework fit surfaces was calculated using the measurements of the mating surfaces. The measuring machine and procedures are similar to those described by Örtorp et al. (169). Using the “least square method”, described by Bühler (188), the position of the framework was superimposed in a “best fit” position onto the abutment replica positions according to the center point positions. The 3D (x-, y-, and z-axis) directions of displacement of the center points were calculated in μm in real and absolute figures. Also, the distortions in angulation misfit were analyzed in X/Z angle and Y/Z angle for all abutment replica positions. Furthermore, using the x-, y-, and z-axis distortions a 3D distortion between the center points of the frameworks and the abutment replicas were calculated for each individual cylinder using the formula ($3D = \sqrt{x^2+y^2+z^2}$) (Figure 11). An identical scanning procedure of the position of the mating surfaces was performed after veneering. To measure the general effect of the ceramic veneering process, the intersecting distances between the center points of implants in positions 1 and 6, positions 2 and 5, and positions 3 and 4, were measured, before and after ceramic veneering, and compared to the distances from the actual model (Figure 12).

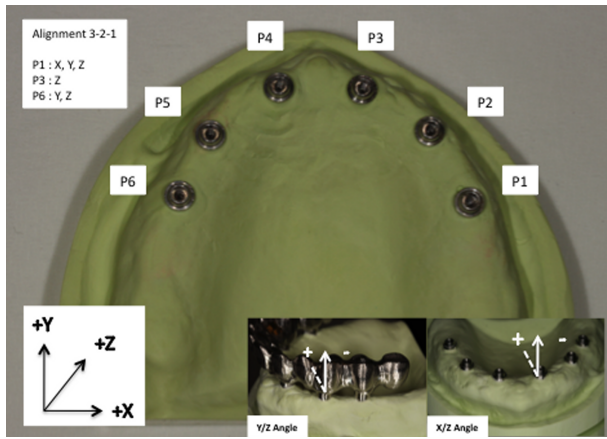


Figure 11. Model with measurement points in x, y, and z-axes for implant positions 1–6.

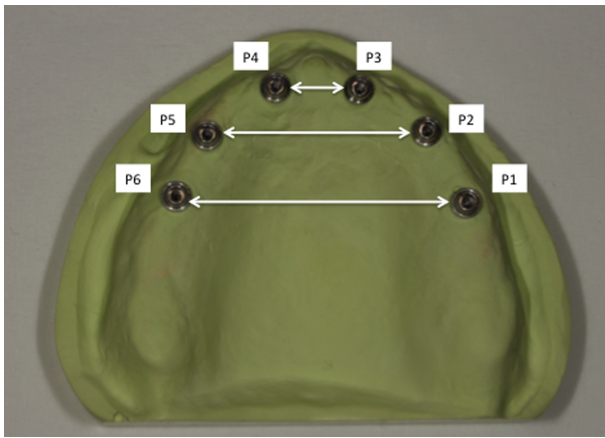


Figure 12. Model with measurement points for distances between implant position 1–6, 2–5, and 3–4.

Five repeated measurements of one stone cast and one framework were conducted to establish the precision of the CMM measurements. The standard deviations of the x, y, and z coordinates for the six implant positions were within $\pm 2\mu\text{m}$.

3.3.6 Statistical analysis

The SPSS (IBM SPSS v.22.0, Chicago, IL, USA) statistics software program was used for statistical analysis. The distribution was analyzed using box-

plots and the parametric paired samples t-test was used to analyze the differences between the frameworks before and after ceramic veneering.

To evaluate the differences between the groups the experiment was regarded as a factorial design in blocks, with models as random blocks and material, production technique and veneering as fixed factors. All two-way interactions between the fixed effects were included in the models. Analysis of variance was used followed by comparisons of interesting contrasts. Calculations were performed with the SAS-procedure MIXED with lsmeans and estimate statements (SAS version 9.3, SAS Institute Inc, Cary, N.C., USA). The assumptions of the tests were checked using residual plots and q-q plots. This was the motivation for logarithmic transformation of data on 3D distortion. For P1–P6 only minor deviations from the assumptions were observed for the original data. The significance level was set at $P < 0.05$.

4 RESULTS

4.1 Part 1. Clinical study on tooth-supported CoCr FDPs (I).

4.1.1 Follow-up

Of 149 patients with 201 FDPs (supported by 743 abutments), 122 patients (82%) with 165 FDPs (82%) (supported by 609 [82%] abutments) were followed up for five years. Twenty-four patients were lost to follow-up (Table 5). Seven FDPs were not followed for five years due to complications; one FDP had a ceramic fracture at time of cementation, one FDP had seven abutment teeth extracted due to caries, one FDP had to be remade due to cement failure and tenderness of an abutment tooth, one FDP was lost due to trauma, and three FDPs had to be shortened to single crowns as a result of cement failure and change of therapy. A patient lost to follow-up could have more than one FDP, and a failed FDP could belong to a patient with another FDP that was considered a success. Therefore, the number of patients lost to follow-up is not coherent with the number of FDPs lost to follow-up. Accordingly, seven FDPs were lost due to complications during the follow-up period and 165 FDPs were followed for five full years.

Table 5. Reasons for patient and CoCr FDP loss to follow-up during the five-year follow-up period. Percentage of total (149 patients, 201 FDPs) is in parentheses.

	Moved/new dentist	Deceased	No contact	Total
Patients (%)	4 (3)	10 (7)	10 (7)	24 (16)
FDPs (%)	4 (2)	14 (7)	11 (5)	29 (14) *

*Further seven FDPs were lost due to complications

4.1.2 Patient Record Registrations

The total number of complications per patient, FDP, and abutment tooth that occurred over five years (including the aforementioned early complications) is presented in table 6. In total, complications occurred in 34 (23%) of 149 patients, 38 (19%) of 201 FDPs, and 60 (8%) of 743 abutment teeth. There were no framework fractures during the follow-up period.

Table 6. Occurrence of complications and failures experienced during five-year follow-up of 201 CoCr FDPs.

Complications	Patient total 149 (%)	FDP total 201 (%)	Abutment teeth total 743 (%)	Failure Survival*	Failure Success [§]
<i>Biological</i>					
Caries	10 (6.7)	10 (5)	16 (2.2)		7
Gingivitis/ mucosal	5 (3.4)	5 (2.5)	9 (1.2)		
Periodontal	3 (2)	4 (2)	7 (0.9)		
Root fillings	7 (4.7)	7 (3.5)	8 (1.1)		5
Extractions ⁺					
periodontal	2 (1.3)	3 (1.5)	6 (0.5)		2
caries	2 (1.3)	2 (1)	8 (0.7)	1	
root fracture	2 (1.3)	2 (1)	2 (0.2)		1
<i>Technical</i>					
Cementation failure	10 (6.7)	10 (5)	23 (3.1)	2	7
Cohesive ceramic fractures	7 (4.7)	7 (3.5)	7 units (8 fractures) (0.7)	1	5
<i>Other</i>					
Tenderness	4 (2.7)	4 (2)	7 (0.9)		
Aesthetic considerations	2 (1.3)	2 (1)	N/A		

⁺One patient had caries complications in one FDP and root fracture in another FDP.

*Shortening of FDP (7), Change of therapy (2).

[§]Change of therapy (2)

None of the eleven FDPs cemented with RelyX lost retention (23 abutments, 9 cantilever pontics, pontic/ abutment ratio: 0.5 [four of the abutments had received root canal treatment before cementation]). Ten (5%) of 190 FDPs cemented with zinc phosphate cement lost retention during the follow-up period. Six of these were cantilever FDPs (28 abutments, 12 distal cantilever pontics, pontic/abutment ratio: 0.5, mean cantilever pontics per FDP: 2, range: 1 to 4 [three shortspan FDPs and three long-span FDPs]) and, among these, four of the abutment teeth involved had received root canal treatment before cementation. Three FDPs were recemented, two were left without intervention (patients did not agree with suggested therapy to recement, FDPs were still in situ), three had a change of therapy (implants), and two were remade. There were no adhesive ceramic fractures. However, for eight (0.7%) of 1,135 units in seven (3.5%) of 201 FDPs, cohesive fractures were registered. Three fractures could simply be polished, one was untreated, three were treated with a corrective composite filling, and one was remade because

of a fracture at cementation. Four of the fractures occurred in the maxilla, four in the mandible, three in the anterior region, and five in the posterior region. Sixteen (2.2%) of 743 abutment teeth in five (3.4%) of 149 patients (seven FDPs) were extracted. The reasons for extraction were periodontal problems related to six (0.5%) of 743 abutment teeth (in two patients), caries in eight (0.7%) of 743 abutment teeth (in two patients), and root fractures in two (0.2%) of 743 abutment teeth (in two patients). Complications occurred in 33% of long-span FDPs (six to 14 units), and 12% of the short-span FDPs (two to five units).

4.1.3 Failures According to Success/Survival Definitions

One hundred forty-seven (73%) of 201 FDPs were considered to be successful according to the success definition. Hence, 29 (14%) FDPs were considered failures. The reasons were: cohesive ceramic fractures (five), cementation failure (seven), abutment teeth extracted (three), root fillings after cementation (five), change of therapy (two), and caries (seven). The remaining 25 FDPs were lost to follow-up (reasons described in table 5). With the definition for survival applied to the material, 160 (80%) of 201 FDPs were considered survivals and 13 (6%) FDPs were considered failures during the five-year follow-up. The reasons were: cohesive ceramic fracture at cementation (one), abutment teeth extracted due to caries (one), cementation failure and tenderness of abutment tooth (one), cementation failure and shortening to a single crown (one), change of therapy (two), and shortening of FDP (seven). FDPs with a cohesive ceramic fracture were considered surviving if repair in the form of a composite correction or polishing was performed. The remaining 28 FDPs were lost to follow-up.

Table 7. Cumulative success rate after five-year follow-up of 201 CoCr FDPs.

CSR= Cumulative success rate %					
Period/year	Examined FDPs	Drop-out	Failed	CSR%	SE
Cementation	201	0	0	100.0	
1	188	5	8	95.7	1.5
2	181	2	5	93.0	1.9
3	167	6	8	88.5	2.4
4	157	7	3	86.8	2.5
5	147	5	5	83.8	2.8
Total	147	25	29	83.8	

The five-year CSRs for success and survival were 83.8% and 92.8%,

respectively (Tables 7 and 8). The actual outcomes of the FDPs with the definitions described by Walton are presented in Table 9.

Table 8. Cumulative survival rate after five-year follow-up of 201 CoCr FDPs.

CSR= Cumulative survival rate %					
Period/year	Examined FDPs	Drop-out	Failed	CSR%	SE
Cementation	201	0	0	100.0	
1	193	5	3	98.4	0.9
2	188	3	2	97.4	1.2
3	178	6	4	95.1	1.6
4	169	7	2	94.0	1.8
5	160	7	2	92.8	1.9
Total	160	28	13	92.8	

Table 9. The six-field classification of the 201 FDPs after five years, according to definitions by Walton (106).

Five-year outcome of CoCr FDPs (n=201)	
Years in service	5
Outcome	%
Success	79
Survival	0
Unknown	10
Dead	6
Repaired	1
Failed	4
Total	100

4.2 Part 2. In vitro study on digital and conventional VPS impressions for tooth-supported FDPs (II).

The conventional VPS impression technique suffered a major complication for one FDP that had to be remade, since the FDP could not be seated on the corresponding study cast due to serious misfit. All FDPs produced with the digital impression technique were easily seated on their study casts. The preset cement spacer settings were identical for both techniques, 30 µm in the cervical area, from the finish line and 0.5mm axially, and 60 µm above the cervical area for the axial and occlusal areas. The mean internal discrepancy

for the FDPs was 117 μm and 93 μm , respectively, for the conventional and digital impression techniques ($p < 0.001$) (Table 10).

Table 10. Mean internal discrepancy in μm and standard deviation (SD) between abutment and inside of FDP produced with conventional and digital impression techniques.

Impression technique	n	Internal discrepancy to master model (μm)					
		Premolar 34		Molar 36		FDP 34–36	
		Mean	(SD)	Mean	(SD)	Mean	(SD)
Conventional VPS	10	100	6.7	127	15.7	117	11.6
Digital	10	91	8.8	95	8.5	93	8.2
Significance (2-tailed) (P<0.01)		0.016		<0.001		<0.001	

Table 11. Absolute marginal discrepancy between finish line and crown margin, for conventional and digital impression techniques.

Impression technique	n	Absolute marginal discrepancy (μm)					
		Premolar 34		Molar 36		FDP 34–36	
		Mean	(SD)	Mean	(SD)	Mean	(SD)
Conventional VPS	10	140	30.9	154	19.0	147	22.6
Digital	10	146	44.5	139	24.7	142	32.6
Significance (2-tailed) (P<0.01)		0.788		0.100		0.425	

Table 12. Cervical area discrepancy for conventional and digital impression techniques.

Impression technique	n	Cervical area discrepancy (μm)					
		Premolar 34		Molar 36		FDP 34–36	
		Mean	(SD)	Mean	(SD)	Mean	(SD)
Conventional VPS	10	61	9.1	77	19.3	69	12.4
Digital	10	44	11.7	44	6.4	44	8.2
Significance (2-tailed) (P<0.01)		0.003		<0.001		0.001	

In general, the distance between the abutment and inner surface of the FDP was the shortest just above the finishing line and the greatest in the occlusal area. The digital impression technique produced FDPs with less discrepancy in the occlusal and cervical area as well as along the axial walls (Figures 13 a-b). The mean absolute marginal discrepancy was 147 μm for the conventional VPS technique and 142 μm for the digital impressions, with no statistically significant difference (Table 11, Figures 14 a-b). The mean cervical area discrepancy was small for both techniques: 44 μm for the digital impression technique and 69 μm for the conventional VPS impression

technique ($p < 0.001$) (Table 12, Figures 15 a-b).

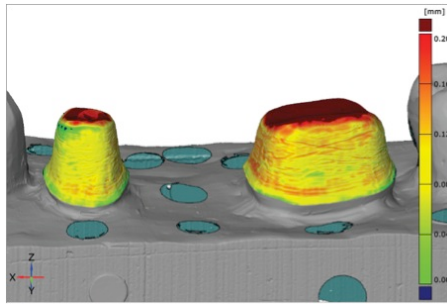


Figure 13 a
Conventional VPS impression

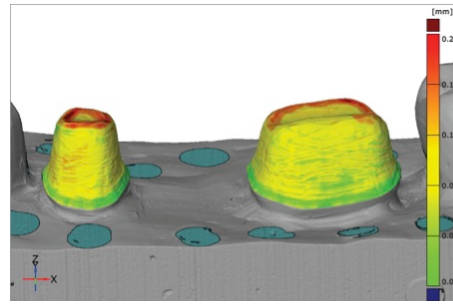


Figure 13 b
Digital impression

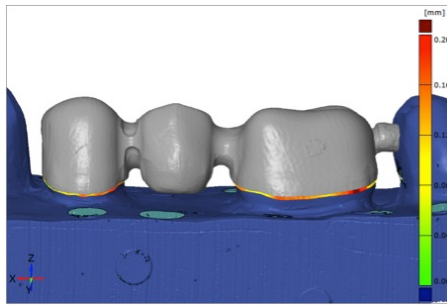


Figure 14 a
Conventional VPS impression

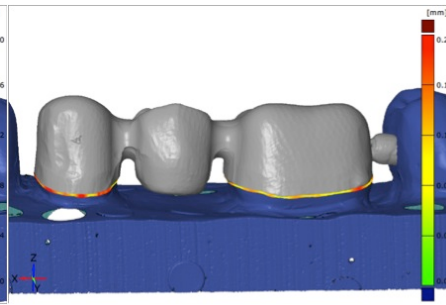


Figure 14 b
Digital impression

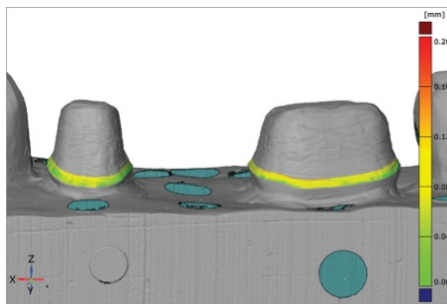


Figure 15 a
Conventional VPS impression

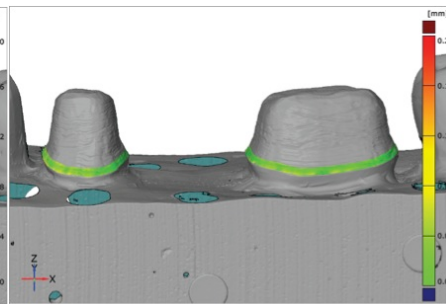


Figure 15 b
Digital impression

4.3 Part 3. In vitro studies on the fit of CNC-milled and additively manufactured CoCr and Ti frameworks for implant-supported FDPs, and the effect of ceramic veneering (III-IV).

4.3.1 Fit results and comparisons within groups before and after ceramic veneering

In the CNC Ti group, the differences in fit after ceramic veneering were statistically significant in the y-axis ($p=0.001$), and the Y/Z angle ($p=0.002$). The changes in intersecting distances between the center point positions were significant for position 1–6 ($p=0.028$), and position 3–4 ($p=0.041$) (Table 13, 14 and 15). For the AM Ti group, the difference in fit in the y-axis ($p=0.002$), and the 3D distortion ($p=0.008$) were statistically significant. The changes in distances between center point positions were statistically significant for position-pairs 1–6 ($p=0.047$), and 3–4 ($p<0.000$). For the CNC CoCr group, statistically significant differences were present in the x-axis ($p=0.001$), the y-axis ($p=0.011$), and in the 3D distortion ($p=0.005$). Statistically significant differences in distance before and after veneering were recorded for positions 1–6 ($p<0.000$), and 2–5 ($p=0.001$). The AM CoCr group showed statistically significant differences in the z-axis ($p=0.011$), the Y/Z angle ($p<0.000$), and the X/Z angle ($p<0.000$) after ceramic veneering. Also, the distances between center point positions were significant for all three position-pairs, 1–6 ($p<0.000$), 2–5 ($p=0.002$), and 3–4 ($p=0.032$).

Table 13. Mean (standard deviation) distortion (in μm) of the center point of the frameworks presented with the master models as references using least square method, in absolute figures.

Material	Veneering	n	/x/	/y/	/z/	3D	95% CI
CNC Ti	Before	10	5.0 (1.5)	2.9 (0.6)	5.2 (2.4)	9.0 (1.5)	7.9; 10.1
CNC Ti	After	10	4.6 (1.8)	4.5 (1.5)	5.4 (2.2)	9.6 (1.9)	8.3; 11.0
AM Ti	Before	10	8.7 (3.3)	7.4 (1.9)	2.4 (0.9)	13.0 (3.3)	10.7; 15.3
AM Ti	After	10	9.4 (2.3)	9.7 (2.2)	2.0 (1.2)	15.0 (3.1)	12.8; 17.2
CNC CoCr	Before	10	13.5 (7.4)	6.3 (3.4)	4.6 (2.8)	17.8 (7.7)	12.3; 23.3
CNC CoCr	After	10	9.7 (6.9)	4.4 (4.0)	4.9 (3.1)	13.7 (7.9)	8.0; 19.3
AM CoCr	Before	10	11.5 (5.0)	7.6 (1.7)	1.6 (0.6)	15.3 (4.6)	12.0; 18.6
AM CoCr	After	10	10.1 (4.2)	7.7 (2.0)	2.2 (0.9)	14.3 (4.0)	11.4; 17.1

n = number of frameworks

CI= confidence interval for mean

Table 14. Mean deviation (standard deviation) in angulation in decimal degrees of the mating surfaces of the frameworks using least square method, in absolute figures.

Material	Veneering	n	X/Z angle		Y/Z angle	
			Mean	SD	Mean	SD
CNC Ti	Before	10	.044	(.030)	.058	(.020)
CNC Ti	After	10	.075	(.034)	.100	(.031)
AM Ti	Before	10	.063	(.050)	.108	(.178)
AM Ti	After	10	.068	(.022)	.089	(.031)
CNC CoCr	Before	10	.061	(.022)	.067	(.026)
CNC CoCr	After	10	.074	(.038)	.068	(.039)
AM CoCr	Before	10	.065	(.021)	.046	(.019)
AM CoCr	After	10	.154	(.036)	.169	(.039)

n = number of frameworks

Table 15. Mean difference (in mm) between the center points of the frameworks after ceramic veneering.

Material	Veneering	n	Center point positions		
			1-6	2-5	3-4
CNC Ti	After	10	-0.007	0.001	0.002
AM Ti	After	10	-0.011	0.003	0.004
CNC CoCr	After	10	-0.020	-0.006	0.000
AM CoCr	After	10	-0.036	-0.012	-0.003

n = number of frameworks

4.3.2 Comparisons between groups

For group comparisons, the variables 3D distortion and distance between center point positions 1-6 were chosen to represent the total fit of the frameworks. An analysis of variance was performed on both variables, for the 3D distortion the fixed factors Material*Production technique and Material*Veneering were found to present significant differences. For the 3D distortion of CoCr, the production technique was non-significant. However, for Ti, the median of 3D distortion was 13.6 μm for the AM technique and 9.1 μm for the CNC technique. The median ratio for the production techniques was 1.48 ($p=0.0001$), meaning that 48% of the difference in 3D distortion within the Ti group can be explained by the production technique (95% CI 1.28-1.72). In the CoCr group, the 3D distortion was significantly different after ceramic veneering, from 15.6 μm to 13.0 μm . The median ratio was 0.83 ($p=0.0163$), meaning that 17% of the difference could be attributed to the veneering process (95% CI 0.72-0.97). For the center point position pair 1-6, the fixed factors Material*Production technique and Material*Veneering presented significant differences. For CoCr, the production technique affected the distance. The AM technique had a shorter distance between center point positions 1-6 compared to the CNC technique

-0.029 mm ($p < 0.001$, 95% CI -0.040 - -0.017). Also, for the CoCr group, the veneering process affected the distance. The distance became shorter after ceramic veneering, -0.028 mm ($p < 0.001$, 95% CI -0.040 – -0.016).

4.3.3 Ceramic veneering experiences

The CNC Ti, CNC CoCr and AM CoCr groups were veneered without complications. The AM Ti group suffered from air bubbles and cracks in the ceramic veneering material in seven of the frameworks, which required adjustments. Seven of the cracks appeared at the surface after a firing cycle and one crack appeared during grinding using a diamond bur (Table 16). Another observation during the ceramic firing procedure was the oxide layer that formed on the Ti frameworks. The oxide layer that formed on the AM Ti frameworks was thicker and more reddish in color compared to the black oxide that formed on the CNC-milled Ti (Figure 16 a-b).

Table 16. Complications during ceramic veneering procedure.

Framework	Complications			
	CNC CoCr	AM CoCr	CNC Ti	AM Ti
1	-	-	-	*
2	-	-	-	** ^u
3	-	-	-	*
4	-	-	-	-
5	-	-	-	°
6	-	-	-	□
7	-	-	-	□□□§
8	-	-	-	-
9	-	-	-	^u §
10	-	-	-	-

* Air bubble

° Crack from bur

^u Crack after 1st firing cycle

□ Crack after 2nd firing cycle

§ Crack after Glaze firing



Figure 16 a
CNC-milled Ti FDP during firing.

Figure 16 b
AM Ti framework during firing.

5 DISCUSSION

5.1 Discussion of materials and methods

5.1.1 Part 1. Clinical study on tooth-supported CoCr FDPs (I).

All patient records were reviewed by two of the authors together, with the experienced prosthodontist as the primary reviewer, after at least five years post cementation. The study was performed in a private clinical setting and two general dentists performed the treatments. Thus the study can be regarded as an effectiveness study in comparison to most published studies that are performed by specialists at university clinics (202) reflecting the efficacy of a treatment modality. The FDPs were manufactured by one dental laboratory, and neither the dental clinic nor the dental laboratory changed materials or manufacturing methods significantly during the study period. Different dental technicians were involved in the stages of manufacturing, casts, frameworks and ceramic veneering. All patients consecutively received CoCr FDPs when an FDP was constructed. Several limitations may be considered, such as the retrospective study design with the information recorded from the patients' dental records without a clinical examination using standardized evaluation criteria. Also, the inclusion of all FDPs irrespective of number of units or position in the arch, and patients could have more than one FDP, which could result in several confounders. Another limitation was the absence of a control group. Instead, the results were compared with similar studies on Au and CoCr alloys (21, 23, 202, 225, 226). Also, the retrospective design may have affected the results due to the possibility of under-reporting of mucosal problems, gingivitis, periodontal problems and ceramic chipping. In contrast, the risk of bias may be low since the decision to evaluate the clinical outcome at the clinic was made five years after the last included FDP had been inserted.

In the present study, the CSR for success and survival were calculated on the FDP level, and the complication percentage was calculated using the full cohort (201 FDPs) including the FDPs that were lost to follow-up. Other studies have used the patient level for CSR and excluded the FDPs that were lost to follow-up when calculating complication percentage. For a better comparison with earlier studies, the CSR for success and survival on the patient level was 80.0% and 91.4% respectively. The complication

percentage using only the FDPs that were followed for five-years or were lost due to complications are presented in table 17.

Table 17. Complications recorded for the FDPs that were followed for five-years or lost due to complications, on both patient and FDP level.

Complications	Based on 149 pat 201 FDPs		Based on 125 pat 173 FDPs	
	Pat (%)	FDP (%)	Pat (%)	FDP (%)
Caries	10 (6.7)	10 (5.0)	8 (6.4)	8 (4.6)
Gingivitis/mucosal	5 (3.4)	5 (2.5)	5 (4.0)	5 (2.9)
Periodontal	3 (2.0)	4 (2.0)	3 (2.4)	4 (2.3)
Root fillings	7 (4.7)	7 (3.5)	7 (5.6)	7 (4.0)
Cementation failure	10 (6.7)	10 (5.0)	10 (8.0)	10 (5.8)
Cohesive ceramic fractures	7 (4.7)	7 (3.5)	7 (5.6)	7 (4.0)
Tenderness	4 (2.7)	4 (2.0)	4 (3.2)	4 (2.3)

5.1.2 Part 2. In vitro study on digital and conventional VPS impressions for tooth-supported FDPs (II).

For fit analysis, the triple-scan protocol using a ATOS scanner was used, the maximum distances obtained with this analysis could be misleading, due to defects in the point cloud that in turn lead to small holes in the CAD file. These defects may occur when scanning the inside of the FDP, because of the triangulation technique. When measuring distances, a hole in the CAD file results in a maximum distance of 400 µm. Thus, a maximum discrepancy of 400 µm may be due to a discrepancy of 400 µm, or to a hole in the point cloud, which implies that the range of the recorded distance may have a false maximum value. However, since these holes are very small they do not affect the overall mean distance calculated from 250.000 to 400.000 points. Also, the triple-scan protocol using the ATOS scanner may not be the most suitable tool for measuring the absolute marginal discrepancy, due to a problem in capturing the outermost thin margin of the FDP. This results in a CAD margin that fails to mirror the physical margin, and therefore the measured discrepancy is larger. To compare the ATOS scanner with a different fit measuring technique the silicon replica technique was used on the test group with the same casts and FDPs. There were no significant differences in the measuring areas internal discrepancy and cervical area discrepancy, but for absolute marginal discrepancy the silicon replica method resulted in a significantly smaller discrepancy. The results using the ATOS scanner was 142 µm, and with the silicon replica technique 94 µm (227).

Stone casts were used as study casts, which could be a confounder because of

dimensional stability, however, no dimensional changes were seen after conventional VPS impression of the stone cast and there were no problems in reproducing the finishing line. In the laboratory setup, no saliva was present, giving optimal conditions for impression taking with both techniques. Whether this favors any of the techniques cannot be established from the present study. Nevertheless, Flügge and colleagues reported that the iTero intraoral scanner produces more precise impressions from stone casts than from patients (228).

During the optical scanning for the fit analysis the FDPs were spray coated with TiO₂ spray, which had a thickness of one to two µm according to the manufacturer. Since both groups of FDPs were sprayed in the same manner and thus were affected in the same way, no difference in fit between the groups should be attributed to the scan spray.

In both the digital and conventional workflow several sources of error are introduced. According to the manufacturer, the accuracy of the iTero intraoral scanner is ±15µm, and is further affected by the material scanned (229, 230). In the conventional workflow, the conditions (dry, moist, wet) during impression taking may affect the dimensional stability and detail reproduction of VPS impressions (231). The process of pouring the stone casts also involves an expansion and contraction of the stone, which could cause a distortion between the prepared teeth and the physical “working” cast (232). In this study, the “working” casts were digitized using a laboratory laser scanner, which, according to the manufacturer has an accuracy of ±10µm (Straumann Cares 2, Straumann, Basel, Switzerland). After digitization, both groups were designed using the Cares CAD software and then manufactured in a CNC-milling machine at a production center (Straumann, Leipzig, Germany). The milling procedure also includes a certain amount of tolerance and causes deviation from the CAD file. Nonetheless, both groups were manufactured using the same technique. The best way of comparing digital and conventional impressions would be to compare the digital impression file with a digitized impression or stone cast using a reference scanner (233). However, in this study, the aim was to compare the fit of three-unit FDPs manufactured using the different techniques, which will inevitably involve all these sources of error that are present in the complete workflow.

5.1.3 Part 3. In vitro studies on the fit of CNC-milled and additively manufactured CoCr and Ti frameworks for implant-supported FDPs, and the effect of ceramic veneering (III-IV).

In this study, a CMM and the “best fit method” for analysis, was used. The “best fit method” matches the coordinates from the model and the framework virtually. The framework is not physically placed on the model for the fit measurements. This method underestimates the distortion in the vertical axis, since the limitations of the physical components are disregarded in the virtual matching (172, 189, 190). Despite this, the CMM method is considered highly accurate when measuring fit of implant-supported FDPs and can record vertical, horizontal and angular distortions (190, 234). Also, five repeated measurements of one of the models and one framework were conducted to measure the precision of the CMM measurements. The standard deviations of the x-, y-, and z-coordinates for the six implant positions were within $\pm 2 \mu\text{m}$. However, all measurements are made in a laboratory, and the appliance cannot be used for measuring fit in the patient. Thus, the results should only be compared with other studies using the same measuring technique. The use of measuring microscopes for measuring vertical discrepancies will inevitably result in a larger registered misfit.

The alloys compared in this study differed in composition, the CNC-milled CoCr contained 7.5% Fe and 16.4% W. The AM CoCr alloy contained 5% Mo and a smaller amount (5.4%,) W, but larger amounts of Co and Cr compared to the CNC-milled CoCr alloy (Table 1). There were small differences in fit between the CNC-milled and AM frameworks before and after ceramic veneering. Since the mating surfaces of the frameworks are milled for both fabrication techniques, the milling equipment and/or the hardness of the material may influence the differences before ceramic veneering. On the other hand the amount and direction of changes of fit after ceramic veneering may depend more on the material composition. The composition of the alloy is important for the material characteristics, such as, resistance to corrosion, strength and ceramic bond strength (235). A study comparing the Vickers hardness (HV) of similar CoCrMo alloys, found the highest hardness in the AM group ($371 \pm 10 \text{ HV}$), followed by cast CoCr with $320 \pm 12 \text{ HV}$, and CNC-milled CoCr with $297 \pm 5 \text{ HV}$ (9). Furthermore, the microstructure, mechanical properties and ion release of an AM CoCrW alloy can be altered using solution heat treatment or by changing the laser strategy during melting (236, 237). In a study by Hedberg et al., the biocompatibility of a CoCrMo alloy manufactured using different AM parameters was compared to cast CoCr. AM CoCr manufactured using a $40 \mu\text{m}$ layer thickness had significantly lower metal release compared to

samples built with 20 μm layers. Also, all AM groups released significantly less metal ions compared to the cast group. The differences were attributed to the melting pools during build, the bigger the melting pool, the bigger grains on the surface of the alloy. Hence, fewer grain boundaries on the surface, also, the grain boundaries in the AM groups were Mo-rich compared to the cast group with Cr-rich boundaries (238). According to the manufacturers, the CoCr alloys in this study follow the requirements in ISO 9693 (Starloy Soft, CNC-milled CoCr), and ISO 13485 as well as ISO 22674:2006 (Renishaw Laser PFM DG1, AM CoCr). Although, there is a lack of clinical follow-up studies with these alloys, the AM CoCr alloy is similar in composition to the more clinically studied Wirobond C alloy (13, 14, 21, 23). A study comparing the corrosion resistance of cast and AM CoCr of the same alloy (Wirobond C+, Bego) before and after ceramic veneering, found that AM CoCr samples had significantly better corrosion resistance after firing compared to cast CoCr, and AM CoCr showed similar corrosion behavior before and after firing at both pH 5 and 2.5 (239). In this study, the FDPs were placed at the abutment level, in a prospective clinical study screw-retained FDPs in CNC-milled CoCr (n 15) and Ti (n 5) on implant level were compared. After one year, there were no significant differences in marginal bone loss between the framework materials (240).

The Ti materials evaluated were also different in composition, the CNC-milled Ti was a CP Ti grade 4 and the AM Ti was a grade 23 alloy (Table 2). The difference in oxide color is most likely due to the oxide thickness and the change in interference of the incident light radiation (241). One important observation during the process of ceramic veneering, was the complications that occurred in the AM Ti group. There is a need for research and testing to optimize the handling and veneering procedures for this group. Studies on thermal oxidation of CP Ti and Ti grade 5 (TiAl6V4) show that time and temperature affects the oxide layer and the oxygen diffusion subzone, high temperatures (above 800°C) causing debonding of the oxide layer (241-243). The TiAl6V4 ELI (grade 23) and TiAl6V4 (grade 5) alloys differs in composition in regard to the content of the interstitial atoms, oxygen, nitrogen and hydrogen. The lower content of oxygen gives the TiAl6V4 ELI alloy lower hardness but increased ductility compared with TiAl6V4 (244).

When veneering a metal framework with ceramics, the framework is subjected to repeated firing cycles that cause oxide to form on the surface. The oxide on the visible metal surfaces and on the implant mating surfaces must be removed using blasting. All frameworks in this study were treated in a similar blasting process, and the z-axis (vertical) distortion change after ceramic veneering was only significant for the AM CoCr frameworks, from 1.6 μm to 2.2 μm . Also, earlier studies have shown that sandblasting of a

CoCr alloy and Ti grade 4 causes comparable amounts of volume loss (62, 245). However, this procedure may be a source of vertical misfit if not carried out correctly. In paper III and IV, the difference in fit after ceramic veneering and subsequent glass bead blasting was minimal. The effect of the blasting procedure was therefore not considered a confounder.

In this study, the fit of the FDPs were evaluated on the same model as was used for fabricating the frameworks. In reality, frameworks will be fabricated from casts made from conventional impressions or a digital file from a digital intraoral impression. This workflow will include sources of error from the different impression techniques. According to a study comparing the distances between scan bodies in digital impressions from different intraoral scanners, there were significant differences between the different scanners. Also, the scanner with the best results between scan bodies 1–3, with placement similar to implant position 1–6 in the present study, had a 23.5 μm larger mean distance compared to the reference model (246).

5.2 Discussion of results

5.2.1 Part 1. Clinical study on tooth-supported CoCr FDPs (I).

This was a five-year retrospective study of 201 CoCr FDPs provided for 149 patients between January 2000 and November 2005. Data were collected following an examination by one of the authors for 165 (82%) of the FDPs in 122 (82%) patients. No framework fractures were reported in this study. Only eight cohesive fractures in seven (0.7%) of 1,135 units, or seven (3.5%) of 201 FDPs were reported, and no adhesive ceramic fractures were found. The registered fracture rate was low compared with other studies on FDPs. In a three- to seven-year clinical evaluation of CoCr FDPs, 17.6% of FDPs had ceramic fractures and 21 (4.4%) of 480 units presented veneer chipping. However, those FDPs were placed in patients with compromised dentitions and the prospective study design allowed for patient evaluations using a strict protocol for function and complications (21). No chipping was reported in a study following AM CoCr single crowns for 47 months (23). In a systematic review of zirconia and Au MC FDPs, a high rate of chipping was reported, with 34% of MC FDPs suffering chipping after three to five years. However, the mean frequency of grade 3 chipping (severe chipping that led to replacement of the entire FDP) was 3.9% (225).

Another systematic review on conventional FDPs and cantilever FDPs estimated the five-year ceramic fracture complication rate for conventional FDPs at 2.9% and cantilever FDPs at 3.5% (202). These clinical results indicate that there is a clear difference in the reported rate of ceramic veneer chipping among studies on both noble alloys and CoCr alloys.

Studies have reported that FDPs with cantilevers are more prone to cement failure (107, 247). In this study, six of ten FDPs that suffered cementation failure were cantilever FDPs. Hence, six (8%) of 79 cantilever FDPs had cement failure compared with four (3%) of 122 non-cantilever FDPs.

Very few gingivitis/mucosal problems were recorded (3.4% of patients, 1.2% of abutment teeth). Although this retrospective study did not record major biologic problems from the gingiva, a potential biologic risk should not be ignored. Several laboratory studies have reported on the elements released from base metal alloys (28). However, conditioning in distilled water has been shown to reduce the elemental release from base metal alloys to the level of high noble alloys, and the amounts of elements released may be well below the estimated daily dietary intake (38). The clinical effect could therefore be less significant. A previous study on CoCr FDPs did not report any adverse reactions to the material (21).

A systematic review revealed that studies on conventional high-noble MC FDPs displayed a five-year survival rate of 93.8% and a five-year success rate of 84.3% (202). The results of the current study (survival rate of 92.8% and success rate of 83.8% after five years) are comparable with conventional high noble FDPs. The most common cause of complications reported in fixed prosthodontics is caries, followed by periapical involvement (248). This is partly supported by the present study, where cementation failure was a complication in ten (6.7%) of 149 patients and 23 (3.1%) of 743 abutment teeth, and caries in ten (6.7%) of 149 patients and 16 (2.2%) of 743 abutment teeth. However, compared to other studies, the occurrence of caries was low (226). This could be attributed to the clinic's recall system to a dental hygienist.

5.2.2 Part 2. In vitro study on digital and conventional VPS impressions for tooth-supported FDPs (II).

The results show that the digital impression technique produced FDPs with a more accurate mean internal and cervical area fit as compared to the conventional VPS impression technique. The CAD software was preset with

a cement spacer gap of 30 μm for the cervical area (the 0.5mm closest to the finishing line) and 60 μm for axial and occlusal areas. In this study, the cervical area discrepancy was 44 μm and 69 μm , respectively, for the digital and conventional VPS impression techniques, which is reasonably close to the preset gap of 30 μm for the digital technique. The digital impression technique could thereby be regarded as more accurate in the critical cervical area. The mean internal discrepancy between abutment and retainer was 93 μm and 117 μm , respectively, for the digital and conventional VPS impression techniques, indicating that the mean internal discrepancy tends to exceed the preset spacer, especially in the occlusal area. However, both impression techniques resulted in an acceptable fit on the axial walls but an increased discrepancy in the occlusal area, especially for the conventional impression technique. The conventional VPS technique also resulted in overall greater variability compared to the digital impression technique, which means that the digital impression technique generated FDPs with higher precision compared to the conventional VPS impression technique regarding internal and cervical area discrepancy.

Earlier studies have reported larger discrepancies in the occlusal area (149, 154, 249) and this is supported by the results in the present study where FDPs produced from the conventional VPS impression technique showed a discrepancy ranging from 160 μm to 400 μm and the digital technique showed discrepancies from 80 μm to 400 μm . However, the maximum value might be smaller than 400 μm since the holes in the point cloud always resulted in a maximum value of 400 μm .

Overall, the mean internal discrepancy for the premolar was slightly smaller than that for the molar with both techniques. A larger occlusal area on the molar might explain this since the occlusal area had greater discrepancies compared to the axial area. When looking at the absolute marginal discrepancy, there was no statistically significant difference in mean value. The results for absolute marginal discrepancy are comparable to earlier studies on milled CoCr and zirconia, 185–260 μm (117) and 94–181 μm (250). The marginal discrepancy measured with this method consists of marginal gap and under- or overextension of the FDP margins. Thus, the results should only be compared to other studies on absolute marginal discrepancy, ideally, only analyzed using the same fit measuring technique.

All of the FDPs produced with the digital impression technique were easily seated on their corresponding study cast. In contrast, one of the FDPs produced with the conventional VPS impression technique could not be seated on the study cast. This was probably due to an inaccurate impression

and/or fabrication of the working cast, since the FDP was easily seated on the working cast.

5.2.3 Part 3. In vitro studies on the fit of CNC-milled and additively manufactured CoCr and Ti frameworks for implant-supported FDPs, and the effect of ceramic veneering (III-IV).

The results showed small distortions of the frameworks in comparison to their corresponding models for all groups, in addition, there were also minor changes in the frameworks after ceramic veneering. The CNC Ti group showed the smallest value in 3D distortion and the CNC CoCr group the highest value before veneering. Interestingly, the Ti groups, increased in 3D distortion after ceramic veneering and the CoCr groups decreased in 3D distortion. For the Ti group, the production technique was a factor that affected the 3D distortion, the AM technique produced frameworks with larger 3D distortion. In the CoCr group, ceramic veneering was a factor that significantly affected the 3D distortion, with a smaller 3D distortion after ceramic veneering. The curvature of the frameworks increased for all four groups, the AM frameworks more than the CNC-milled frameworks and the CoCr frameworks more than the Ti frameworks. For the CoCr frameworks, both production technique and ceramic veneering were factors that affected the curvature. The curvature was larger in frameworks produced with the AM technique, also the curvature in all frameworks increased after ceramic veneering. The hypothesis in paper III and IV, that there would be no difference in fit among the groups before ceramic veneering was rejected. The hypothesis in paper III, that the fit of CNC-milled CoCr frameworks would be similar to the fit of Ti frameworks while being unaffected by ceramic veneering was rejected. In paper IV, the hypothesis that there would be a difference in fit before and after ceramic veneering within the groups was accepted.

Even though there were statistically significant differences within and among the groups, it must be clearly stated that the results are well within what may be regarded as clinically accepted. The single framework with the largest 3D distortion was a CNC CoCr framework with a mean 3D distortion of 37.7 μm before ceramic veneering. Earlier publications have discussed misfit and the importance of “passive fit”, without consensus (189, 197-199). Suggestions of levels of misfit for clinical acceptability have been presented for the vertical (z-axis) distortion, from 40 μm up to 150 μm (179, 251). In the present study, the framework with the largest vertical distortion was still below 9 μm .

Usually, studies on implant frameworks are conducted on implants placed in the mandible, where the curvature of the frameworks is less pronounced. In the study by Örtorp et al., the distance between the terminal implants was 30.9 mm (169). In studies on frameworks for the maxilla, the arch is larger as in the present study, and the frameworks showed a distance between the distal implants (positions 1–6) of 40.5 mm. A similar distance was reported by Katsoulis et al. (252), investigating frameworks fabricated for the maxilla with a distance of 40 mm between the terminal implants. Theoretically, the veneering process might therefore affect frameworks for the maxilla more than frameworks for the mandible. However, this has not been confirmed.

The effect of ceramic veneering of Ti (CP grade 2) frameworks on the fit of implant-supported FDPs has been studied by Örtorp et al. (169), who used a CMM to analyze the fit, reporting no significant change in fit by the veneering process. These results were confirmed by Katsoulis et al. (CP grade 4) (252), measuring the vertical fit using the one-screw fit test and a scanning electron microscope. Tiozzi et al. (218), comparing Ti (CP grade 1) and CoCr in three-unit implant-supported FDPs before and after simulated ceramic firings and using the one-screw fit test and an optical microscope to measure vertical misfit, reported no significant differences. This is in accordance with the results for vertical misfit for the Ti and CoCr frameworks in the present study where only the AM CoCr group presented a statistically significant increase in z-axis after ceramic veneering. However, the difference for AM CoCr changed from 1.6 μm to 2.2 μm and was among the smallest distortions compared to the other groups. Fonseca et al. (137) studied marginal fit of tooth-supported single crowns after simulated ceramic firings, using a travelling microscope, and all three materials (CP Ti grade 2, Ti6Al4V alloy, and PdAg alloy) were negatively affected by the firing procedures, with significant increases in marginal discrepancies. The reason for this difference in recorded distortion after heat cycles could be the thin cervical margins on tooth-supported crowns as compared with the thick framework dimension in implant FDPs where no veneering material is applied close to the mating surfaces. The clinical relevance of misfit in implant-supported FDP is debated, where some studies claim that misfit is detrimental to the surrounding bone, whereas others suggest that it is favorable and stimulates bone remodeling (196-199, 201). Concerning the technical relevance of misfit, several studies argue that FDP misfit is related to screw complications (253-256). Thus, it is clear that a good framework fit should be strived for.

With the introduction of CAD/CAM techniques in fabrication of implant frameworks, the fit of prostheses has improved. Although passive fit of

implant frameworks has not been achieved yet, the improvement especially in the vertical fit may result in a decrease of screw loosening events. FEA studies have shown that increased stiffness in frameworks with misfit increases the risk of mechanical failures (257). However, one can only speculate whether the difference in stiffness of material, CoCr as compared with Au and Ti, may have an impact on the risk of screw loosening for frameworks with minor misfit. According to an FEA study, the stress in the retaining screw decreased for stiffer framework materials with a vertical misfit of 10 and 50 μm (258). Earlier clinical studies have reported an increase of screw loosening in frameworks with a misfit larger than 150 μm . A clinical study evaluating frameworks after an average of 19 years of clinical use using an optical scanner and the “best-fit” method for analysis reported an overall misfit of the frameworks of 150 μm (range 95–232 μm) and stated that the effect misfit had on the long-term clinical outcome was minor (259). In the present study, frameworks had a mean vertical misfit of less than 10 μm . The present CAD/CAM techniques used for framework fabrication produces frameworks with a fit superior to cast frameworks and may therefore contribute to further reduction in technical complications for implant-supported FDPs.

6 CONCLUSIONS

CoCr FDPs are a promising prosthodontic alternative to other dental alloys, presenting a low level of ceramic fractures, cement failure, caries, and other complications during the first five years in function. To evaluate their longer-term success and possible biologic adverse effects, further long-term randomized controlled studies are necessary. The research hypothesis that CoCr FDPs function well in a clinical setting during a follow-up period of five years was accepted.

It can be concluded, that in a laboratory test situation the digital impression technique was more accurate than conventional impressions using VPS impression material. The null hypothesis was therefore rejected and the alternative hypothesis was accepted, since the digital impression technique produced FDPs with a significantly closer fit.

Implant-supported frameworks can be produced in either Ti or CoCr using either CNC-milling or additive manufacturing with a fit well within the range of what is regarded as clinically acceptable. The fit of frameworks of both materials and production techniques are affected by the ceramic veneering procedure to a small extent, most likely of no clinical significance.

7 FUTURE PERSPECTIVES

The clinical retrospective study was based on CoCr FDPs manufactured using the lost wax technique. It may be hypothesized that recent developments in CAD/CAM dentistry may further improve the clinical results due to a more controlled workflow. It was shown in this thesis that the new manufacturing techniques that have been introduced to dentistry, such as; digital impressions, the CNC-milling technique, and additive manufacturing, seems promising and could improve dental treatments by providing more accurate restorations with less remakes, less complications and improved patient comfort as a result. Also, the economical and environmental benefits due to fewer transports between clinic and laboratory, and less material use should not be neglected.

The fit of the tooth-supported three-unit FDPs was good and with a cervical area discrepancy of 44 μm for the digital and 69 μm for the conventional technique they would all be regarded as clinically acceptable. The triple-scan protocol for 3D fit assessment can be used to measure the accuracy of fit of tooth-supported FDPs as it provides a good 3D measurement of all surfaces with the exception of assessing the absolute marginal discrepancy. However, further clinical studies are needed to confirm that comparable results can be achieved in vivo on small and large-span FDPs.

In the future, a 3D analysis of fit of the framework in the clinic might be performed with an intraoral scanner provided with a quality control software. In a recent publication, Jokstad and Shokati used an intraoral scanner combined with a laboratory scanner and software to assess clinical misfit of implant-supported FDPs (259).

With the increased use of new manufacturing techniques, new materials are being introduced in dentistry or used for new applications/indications. These materials need to be evaluated, e.g. further studies are needed to evaluate the thermal oxidation behavior of TiAl6V4 ELI, and the biological impact of these materials on the human body.

ACKNOWLEDGEMENT

I would like to express my sincere gratitude to everyone who has been involved in the work with this thesis, in particular:

Anders Örtorp, my main supervisor and co-author, for inspiration, guidance and support

Victoria Stenport, my main supervisor and co-author, for guidance and support

Alf Eliasson, my co-supervisor and co-author, for expertise and guidance.

My co-supervisors, Stig Karlsson and Torsten Jemt

My co-authors: Lena Längström, Ritva Moiso Lundh, Göran Bjerkstig, Henrik Skjerven and Pablo Carlsson

My colleagues and staff at the department of prosthodontics/dental materials science and everyone involved in the program of dental technology

Gunnar E Carlsson for consultation regarding manuscript

Kjell Pettersson and Anders Magnuson are acknowledged for statistical support

The staff at Arvidsson`s dental laboratory, the dental clinic of Drs Lundh and Längström, Cascade, Mylab, Straumann, Dentsply Sirona, and TIC/DP Dental laboratory in Gothenburg are gratefully acknowledged for their support

And most of all to my family and friends

This thesis was supported financially in part by grants from the Wilhelm and Martina Lundgren Science Foundation, the Adlerbert Research Foundation, Public Dental Health Service Örebro County Council, the Hjalmar Svenssons Foundation, the Sylvan Foundation, Straumann, Dentsply Sirona Implants, IIS grant I-IS-15-057, and GC Nordic.

REFERENCES

1. Anusavice KJ, Cascone P. Dental casting and soldering alloys. In: Anusavice KJ, editor. *Phillips' science of dental materials*. 11. St. Louis: Saunders; 2003. p. 566.
2. Wataha JC. Alloys for prosthodontic restorations. *J Prosthet Dent*. 2002;87:351-63.
3. Kelly JR, Rose TC. Nonprecious alloys for use in fixed prosthodontics: a literature review. *J Prosthet Dent*. 1983;49:363-70.
4. Leinfelder KF. An evaluation of casting alloys used for restorative procedures. *J Am Dent Assoc*. 1997;128:37-45.
5. Bezzon OL, Pedrazzi H, Zaniquelli O, da Silva TB. Effect of casting technique on surface roughness and consequent mass loss after polishing of NiCr and CoCr base metal alloys: a comparative study with titanium. *J Prosthet Dent*. 2004;92:274-7.
6. Beuer F, Schweiger J, Edelhoff D. Digital dentistry: an overview of recent developments for CAD/CAM generated restorations. *Br dent J*. 2008;204:505-11.
7. Touchstone A, Nieting T, Ulmer N. Digital transition: the collaboration between dentists and laboratory technicians on CAD/CAM restorations. *J Am Dent Assoc*. 2010;141:15-9.
8. Koutsoukis T, Zinelis S, Eliades G, Al-Wazzan K, Rifaiy MA, Al Jabbari YS. Selective Laser Melting Technique of Co-Cr Dental Alloys: A Review of Structure and Properties and Comparative Analysis with Other Available Techniques. *J Prosthodont*. 2015;24(4):303-12.
9. Al Jabbari YS, Koutsoukis T, Barmpagadaki X, Zinelis S. Metallurgical and interfacial characterization of PFM Co-Cr dental alloys fabricated via casting, milling or selective laser melting. *Dent Mater*. 2014;30(4):e79-88.
10. Wu L, Zhu H, Gai X, Wang Y. Evaluation of the mechanical properties and porcelain bond strength of cobalt-chromium dental alloy fabricated by selective laser melting. *J Prosthet Dent*. 2014;111(1):51-5.
11. Sertgoz A. Finite element analysis study of the effect of superstructure material on stress distribution in an implant-supported fixed prosthesis. *Int J Prosthodont*. 1997;10(1):19-27.
12. Teigen K, Jokstad A. Dental implant suprastructures using cobalt–chromium alloy compared with gold alloy framework veneered with ceramic or acrylic resin: a retrospective cohort study up to 18 years. *Clin Oral Implants Res*. 2012;23(7):853-60.
13. Ortorp A, Ascher A, Svanborg P. A 5-year retrospective study of cobalt-chromium-based single crowns inserted in a private practice. *Int J Prosthodont*. 2012;25(5):480-3.

14. Svanborg P, Langstrom L, Lundh RM, Bjerkstig G, Ortorp A. A 5-year retrospective study of cobalt-chromium-based fixed dental prostheses. *Int J Prosthodont.* 2013;26(4):343-9.
15. Anusavice KJ. Structure and properties of cast dental alloys. In: Anusavice KJS, C. Rawls, H. R., editor. *Phillips' science of dental materials.* 12. St. Louis: Saunders; 2013. p. 71.
16. Shen C. Dental casting alloys and metal joining. In: Anusavice KJS, C. Rawls, H. R., editor. *Phillips' science of dental materials.* 12. St. Louis: Saunders; 2013. p. 376-7.
17. Niinomi M. Mechanical properties of biomedical titanium alloys. *Mat Sci Eng A.* 1998;243(1):231-6.
18. McCracken M. Dental implant materials: commercially pure titanium and titanium alloys. *J Prosthodont.* 1999;8(1):40-3.
19. Rack HJ, Qazi J. Titanium alloys for biomedical applications. *Mater Sci Eng C.* 2006;26(8):1269-77.
20. Williams DF. On the mechanisms of biocompatibility. *Biomaterials.* 2008;29(20):2941-53.
21. Eliasson A, Arnelund CF, Johansson A. A clinical evaluation of cobalt-chromium metal-ceramic fixed partial dentures and crowns: A three- to seven-year retrospective study. *J Prosthet Dent.* 2007;98:6-16.
22. Hjalmarsson L, Smedberg J, Pettersson M, Jemt T. Implant-Level Prostheses in the Edentulous Maxilla: A Comparison with Conventional Abutment-Level Prostheses After 5 Years of Use. *Int J Prosthodont.* 2011;24:158-67.
23. Tara MA, Eschbach S, Bohlsen F, Kern M. Clinical outcome of metal-ceramic crowns fabricated with laser-sintering technology. *Int J Prosthodont.* 2011;24:46-8.
24. Hultström M, Nilsson U. Cobalt-chromium as a framework material in implant-supported fixed prostheses: a preliminary report. *Int J Oral Maxillofac Implants.* 1990;6(4):475-80.
25. Geurtsen W. Biocompatibility of dental casting alloys. *Crit Rev Oral Biol Med.* 2002;13:71-84.
26. Tai Y, De Long R, Goodkind RJ, Douglas WH. Leaching of nickel, chromium, and beryllium ions from base metal alloy in an artificial oral environment. *J Prosthet Dent.* 1992;68:692-7.
27. Ardlin BI, Dahl JE, Tibballs JE. Static immersion and irritation tests of dental metal-ceramic alloys. *Eur J Oral Sci.* 2005;113:83-9.
28. Al-Hiyasat AS, Bashabsheh OM, Darmani H. Elements released from dental casting alloys and their cytotoxic effects. *Int J Prosthodont.* 2002;15:473-8.
29. Stenberg T. Release of cobalt from cobalt chromium alloy constructions in the oral cavity of man. *Scandinavian journal of dental research.* 1982;90(6):472-9.
30. Schmalz G, Garhammer P. Biological interactions of dental cast alloys with oral tissues. *Dent Mater.* 2002;18:396-406.

31. Hensten-Pettersen A. Casting alloys: side-effects. *Adv Dent Res.* 1992;6:38-43.
32. Al-Hiyasat AS, Bashabsheh OM, Darmani H. An investigation of the cytotoxic effects of dental casting alloys. *Int J Prosthodont.* 2003;16(1):8-12.
33. Kettelarij JA, Liden C, Axen E, Julander A. Cobalt, nickel and chromium release from dental tools and alloys. *Contact Dermatitis.* 2014;70(1):3-10.
34. Burgaz S, Demircigil GC, Yilmazer M, Ertas N, Kemaloglu Y, Burgaz Y. Assessment of cytogenetic damage in lymphocytes and in exfoliated nasal cells of dental laboratory technicians exposed to chromium, cobalt, and nickel. *Mutat Res.* 2002;521(1-2):47-56.
35. Selden AI, Persson B, Bornberger-Dankvardt SI, Winstrom LE, Bodin LS. Exposure to cobalt chromium dust and lung disorders in dental technicians. *Thorax.* 1995;50(7):769-72.
36. Selden A, Sahle W, Johansson L, Sorenson S, Persson B. Three cases of dental technician's pneumoconiosis related to cobalt-chromium-molybdenum dust exposure. *Chest.* 1996;109(3):837-42.
37. Viennot S, Dalard F, Lissac M, Grosogeat B. Corrosion resistance of cobalt-chromium and palladium-silver alloys used in fixed prosthetic restorations. *Eur J Oral Sci.* 2005;113:90-5.
38. Geis-Gerstorfer J, Sauer KH, Passler K. Ion release from Ni-Cr-Mo and Co-Cr-Mo casting alloys. *Int J Prosthodont.* 1991;4:152-8.
39. Shi L, Northwood DO, Cao Z. The properties of a wrought biomedical cobalt-chromium alloy. *J Mater Sci.* 1994;29(5):1233-8.
40. Kasemo BL, J. Metal selection and surface characteristics. In: Brånemark P-IZ, G.A. Albrektsson, T., editor. *Tissue-integrated prostheses.* Chicago, Illinois: Quintessence Publishing Co., Inc.; 1985. p. 99-116.
41. Kasemo B. Biocompatibility of titanium implants: surface science aspects. *J Prosthet Dent.* 1983;49(6):832-7.
42. Branemark P-I. Osseointegration and its experimental background. *J Prosthet Dent.* 1983;50(3):399-410.
43. Brånemark P-IH, B. Adell, R. Breine, U. Lindström, J. Hallén, O. Öhman, A. Osseointegrated implants in the treatment of the edentulous jaw. Experience from a 10-year period. Stockholm, Sweden: Almqvist & Wiksell International; 1977.
44. Adell R, Eriksson B, Lekholm U, Branemark PI, Jemt T. Long-term follow-up study of osseointegrated implants in the treatment of totally edentulous jaws. *Int J Oral Maxillofac Implants.* 1990;5(4):347-59.
45. Adell R, Lekholm U, Rockler B, Brånemark P-I. A 15-year study of osseointegrated implants in the treatment of the edentulous jaw. *Int J Oral Surg.* 1981;10(6):387-416.
46. Jemt T, Olsson M, Franke Stenport V. Incidence of First Implant Failure: A Retrospective Study of 27 Years of Implant Operations

- at One Specialist Clinic. *Clin Implant Dent Relat Res.* 2015;17 Suppl 2:e501-10.
47. Strietzel R, Hösch A, Kalbfleisch H, Buch D. In vitro corrosion of titanium. *Biomaterials.* 1998;19(16):1495-9.
48. Kuphasuk C, Oshida Y, Andres CJ, Hovijitra ST, Barco MT, Brown DT. Electrochemical corrosion of titanium and titanium-based alloys. *J Prosthet Dent.* 2001;85(2):195-202.
49. Park Y-J, Song Y-H, An J-H, Song H-J, Anusavice KJ. Cytocompatibility of pure metals and experimental binary titanium alloys for implant materials. *J Dent.* 2013;41(12):1251-8.
50. Lövgren R, Andersson B, Carlsson GE, Ödman P. Prospective clinical 5-year study of ceramic-veneered titanium restorations with the Procera system. *J Prosthet Dent.* 2000;84(5):514-21.
51. Ortorp A, Jemt T. Clinical experiences with laser-welded titanium frameworks supported by implants in the edentulous mandible: a 10-year follow-up study. *Clin Implant Dent Relat Res.* 2006;8(4):198-209.
52. Ortorp A, Jemt T. Clinical experiences of computer numeric control-milled titanium frameworks supported by implants in the edentulous jaw: a 5-year prospective study. *Clin Implant Dent Relat Res.* 2004;6(4):199-209.
53. Kaus T, Probst L, Weber H. Clinical follow-up study of ceramic veneered titanium restorations--three-year results. *Int J Prosthodont.* 1996;9(1):9-15.
54. Anusavice KJ. Dental Ceramics. In: Anusavice KJ, C. Rawls, H. R., editor. *Phillips' science of dental materials.* 12. St. Louis: Saunders; 2013. p. 434-5.
55. Baran GR. Phase changes in base metal alloys along metal-porcelain interfaces. *J Dent Res.* 1979;58(11):2095-104.
56. McLean JW. Evolution of dental ceramics in the twentieth century. *J Prosthet Dent.* 2001;85(1):61-6.
57. Schierano G, Bassi F, Audenino G, Pera P, Carossa S. Bond between gold alloy and ceramic in relation to the thickness of the oxide layer. *Minerva stomatologica.* 1999;48(12):577-83.
58. Anusavice KJ. Dental Ceramics. In: Anusavice KJ, C. Rawls, H. R., editor. *Phillips' science of dental materials.* 12. St. Louis: Saunders; 2013. p. 437.
59. Naylor W. How does dental porcelain bond to metal? *Introduction to metal ceramic technology.* Carol Stream, Illinois: Quintessence Publishing Co; 1992. p. 83-91.
60. Lombardo G, Nishioka R, Souza R, Michida S, Kojima A, Mesquita A, et al. Influence of surface treatment on the shear bond strength of ceramics fused to cobalt-chromium. *J Prosthodont.* 2010;19(2):103-11.
61. de Vasconcellos LGO, Silva LH, Reis de Vasconcellos LM, Balducci I, Takahashi FE, Bottino MA. Effect of airborne-particle abrasion

- and mechanico-thermal cycling on the flexural strength of glass ceramic fused to gold or cobalt-chromium alloy. *J Prosthodont.* 2011;20(7):553-60.
62. Kern M, Thompson VP. Sandblasting and silica-coating of dental alloys: volume loss, morphology and changes in the surface composition. *Dent Mater.* 1993;9(3):151-61.
63. ISO. ISO Standard 9693-1. Dentistry—compatibility testing—part 1: metal-ceramic systems. Geneva, Switzerland: International Organization for Standardization; 2012.
64. Berry J, Nesbit M, Saberi S, Petridis H. Communication methods and production techniques in fixed prosthesis fabrication: a UK based survey. Part 2: production techniques. *Br Dent J.* 2014;217(6):E13.
65. Uusalo EK, Lassila VP, Yli-Urpo AU. Bonding of dental porcelain to ceramic-metal alloys. *J Prosthet Dent.* 1987;57(1):26-9.
66. Wu Y, Moser JB, Jameson LM, Malone WF. The effect of oxidation heat treatment of porcelain bond strength in selected base metal alloys. *J Prosthet Dent.* 1991;66:439-44.
67. Mackert JR, Jr., Parry EE, Hashinger DT, Fairhurst CW. Measurement of oxide adherence to PFM alloys. *J Dent Res.* 1984;63:1335-40.
68. Minesaki Y, Murahara S, Kajihara Y, Takenouchi Y, Tanaka T, Suzuki S, et al. Effect of metal conditioner on bonding of porcelain to cobalt-chromium alloy. *J Adv Prosthodont.* 2016;8(1):1-8.
69. Li J, Ye X, Li B, Liao J, Zhuang P, Ye J. Effect of oxidation heat treatment on the bond strength between a ceramic and cast and milled cobalt-chromium alloys. *Eur J Oral Sci.* 2015;123(4):297-304.
70. Bae EJ, Kim JH, Kim WC, Kim HY. Bond and fracture strength of metal-ceramic restorations formed by selective laser sintering. *J Adv Prosthodont.* 2014;6(4):266-71.
71. Vidotti HA, Pereira JR, Insaurralde E, de Almeida AL, do Valle AL. Thermo and mechanical cycling and veneering method do not influence Y-TZP core/veneer interface bond strength. *J Dent.* 2013;41(4):307-12.
72. Pretti M, Hilgert E, Bottino MA, Avelar RP. Evaluation of the shear bond strength of the union between two CoCr-alloys and a dental ceramic. *J Appl Oral Sci.* 2004;12(4):280-4.
73. Lee DH, Lee BJ, Kim SH, Lee KB. Shear bond strength of porcelain to a new millable alloy and a conventional castable alloy. *J Prosthet Dent.* 2015;113(4):329-35.
74. de Melo RM, Travassos AC, Neisser MP. Shear bond strengths of a ceramic system to alternative metal alloys. *J Prosthet Dent.* 2005;93(1):64-9.
75. Serra-Prat J, Cano-Batalla J, Cabratosa-Termes J, Figueras-Àlvarez O. Adhesion of dental porcelain to cast, milled, and laser-sintered cobalt-chromium alloys: Shear bond strength and sensitivity to thermocycling. *J Prosthet Dent.* 2014.

76. Joias RM, Tango RN, Junho de Araujo JE, Junho de Araujo MA, Ferreira Anzaloni Saavedra Gde S, Paes-Junior TJ, et al. Shear bond strength of a ceramic to Co-Cr alloys. *J Prosthet Dent.* 2008;99(1):54-9.
77. Akova T, Ucar Y, Tukay A, Balkaya MC, Brantley WA. Comparison of the bond strength of laser-sintered and cast base metal dental alloys to porcelain. *Dent Mater.* 2008;24(10):1400-4.
78. Suleiman SH, Vult von Steyern P. Fracture strength of porcelain fused to metal crowns made of cast, milled or laser-sintered cobalt-chromium. *Acta Odontol Scand.* 2013;71(5):1280-9.
79. Chan KS, Koike M, Johnson BW, Okabe T. Modeling of alpha-case formation and its effects on the mechanical properties of titanium alloy castings. *Metall Mater Trans A.* 2008;39(1):171-80.
80. Adachi M, Mackert JR, Jr., Parry EE, Fairhurst CW. Oxide adherence and porcelain bonding to titanium and Ti-6Al-4V alloy. *J Dent Res.* 1990;69(6):1230-5.
81. Ozcan I, Uysal H. Effects of silicon coating on bond strength of two different titanium ceramic to titanium. *Dent Mater.* 2005;21(8):773-9.
82. Lin MC, Huang HH. Improvement in dental porcelain bonding to milled, noncast titanium surfaces by gold sputter coating. *J Prosthodont.* 2014;23(7):540-8.
83. Zhao CQ, Wu SQ, Lu YJ, Gan YL, Guo S, Lin JJ, et al. Evaluation to the effect of B₂O₃-La₂O₃-SrO-Na₂O-Al₂O₃ bonding agent on Ti6Al4V-porcelain bonding. *J Mech Behav Biomed Mater.* 2016;63:75-85.
84. Tholey MJ, Waddell JN, Swain MV. Influence of the bonder on the adhesion of porcelain to machined titanium as determined by the strain energy release rate. *Dent Mater.* 2007;23(7):822-8.
85. Park S, Kim Y, Kim H, Lim H, Oh G, Ong JL, et al. Gold and titanium nitride coatings on cast and machined commercially pure titanium to improve titanium-porcelain adhesion. *Surf Coat Tech.* 2009;203(20):3243-9.
86. Vasquez VZ, Ozcan M, Kimpara ET. Evaluation of interface characterization and adhesion of glass ceramics to commercially pure titanium and gold alloy after thermal- and mechanical-loading. *Dent Mater.* 2009;25(2):221-31.
87. Haag P, Nilner K. Bonding between titanium and dental porcelain: A systematic review. *Acta Odontol Scand.* 2010.
88. Naylor W. Essentials of metal ceramic substructure design. *Introduction to metal ceramic technology.* Carol Stream, Illinois: Quintessence Publishing Co; 1992. p. 43-64.
89. Naylor W. Fundamentals of spruing, investing, and casting. *Introduction to metal ceramic technology.* Carol Stream, Illinois: Quintessence Publishing Co; 1992. p. 65-81.
90. Naylor W. Preparation of the metal substructure for porcelain. *Introduction to metal ceramic technology.* Carol Stream, Illinois: Quintessence Publishing Co; 1992. p. 93-105.

91. Shen C. Dental casting alloys and metal joining. In: Anusavice KJS, C. Rawls, H. R., editor. *Phillips' science of dental materials*. 12. St. Louis: Saunders; 2013. p. 387.
92. Willer J, Rossbach A, Weber HP. Computer-assisted milling of dental restorations using a new CAD/CAM data acquisition system. *J Prosthet Dent*. 1998;80(3):346-53.
93. Liu Q, Leu MC, Schmitt SM. Rapid prototyping in dentistry: technology and application. *Int J Adv Manuf Tech*. 2006;29(3):317-35.
94. Murr LE, Gaytan SM, Ramirez DA, Martinez E, Hernandez J, Amato KN, et al. Metal Fabrication by Additive Manufacturing Using Laser and Electron Beam Melting Technologies. *J Mater Sci Technol*. 2012;28(1):1-14.
95. Vandenbroucke B, Kruth JP. Selective laser melting of biocompatible metals for rapid manufacturing of medical parts. *Rapid Prototyping J*. 2007;13(4):196-203.
96. Guo N, Leu MC. Additive manufacturing: technology, applications and research needs. *Front Mech Eng*. 2013;8(3):215-43.
97. Lagutkin S, Achelis L, Sheikhaliev S, Uhlenwinkel V, Srivastava V. Atomization process for metal powder. *Mat Sci Eng A*. 2004;383(1):1-6.
98. Antony LV, Reddy RG. Processes for production of high-purity metal powders. *JOM*. 2003;55(3):14-8.
99. Singh D, Dangwal S. Effects of process parameters on surface morphology of metal powders produced by free fall gas atomization. *J Mater Sci*. 2006;41(12):3853-60.
100. Kruth JP, Mercelis P, Van Vaerenbergh J, Froyen L, Rombouts M. Binding mechanisms in selective laser sintering and selective laser melting. *Rapid Prototyping J*. 2005;11(1):26-36.
101. Ayyildiz S, Soylu EH, Ide S, Kilic S, Sipahi C, Piskin B, et al. Annealing of Co-Cr dental alloy: effects on nanostructure and Rockwell hardness. *J Adv Prosthodont*. 2013;5(4):471-8.
102. Ender A, Mehl A. Full arch scans: conventional versus digital impressions--an in-vitro study. *Int J Comput Dent*. 2011;14(1):11-21.
103. Persson AS, Andersson M, Oden A, Sandborgh-Englund G. Computer aided analysis of digitized dental stone replicas by dental CAD/CAM technology. *Dent Mater*. 2008;24(8):1123-30.
104. Brunette DM. *Critical thinking: Understanding and evaluating dental research*. Carol Stream, IL, USA: Quintessence Publishing Co, Inc; 1996.
105. *A Dictionary of Mechanical Engineering*. 'Oxford University Press'. Precision.
106. Walton TR. An up to 15-year longitudinal study of 515 metal-ceramic FPDs: Part 1. Outcome. *Int J Prosthodont*. 2002;15:439-45.
107. Karlsson S. A clinical evaluation of fixed bridges, 10 years following insertion. *J Oral Rehabil*. 1986;13:423-32.

108. Shillingburg HT, Jr., Hobo S, Fisher DW. Preparation design and margin distortion in porcelain-fused-to-metal restorations. *J Prosthet Dent.* 1973;29(3):276-84.
109. Molin MK, Karlsson SL. Five-year clinical prospective evaluation of zirconia-based Denzir 3-unit FPDs. *Int J Prosthodont.* 2008;21(3):223-7.
110. Monaco C, Caldari M, Scotti R, Group ACR. Clinical evaluation of 1,132 zirconia-based single crowns: a retrospective cohort study from the AIOP clinical research group. *Int J Prosthodont.* 2013;26(5):435-42.
111. Makarouna M, Ullmann K, Lazarek K, Boening KW. Six-year clinical performance of lithium disilicate fixed partial dentures. *Int J Prosthodont.* 2011;24(3):204-6.
112. Sola-Ruiz MF, Lagos-Flores E, Roman-Rodriguez JL, Highsmith Jdel R, Fons-Font A, Granell-Ruiz M. Survival rates of a lithium disilicate-based core ceramic for three-unit esthetic fixed partial dentures: a 10-year prospective study. *Int J Prosthodont.* 2013;26(2):175-80.
113. Holmes JR, Bayne SC, Holland GA, Sulik WD. Considerations in measurement of marginal fit. *J Prosthet Dent.* 1989;62(4):405-8.
114. Colpani JT, Borba M, Della Bona A. Evaluation of marginal and internal fit of ceramic crown copings. *Dent Mater.* 2013;29(2):174-80.
115. Beuer F, Aggstaller H, Richter J, Edelhoff D, Gernet W. Influence of preparation angle on marginal and internal fit of CAD/CAM-fabricated zirconia crown copings. *Quintessence Int.* 2009;40(3):243-50.
116. Sorensen JA. A standardized method for determination of crown margin fidelity. *J Prosthet Dent.* 1990;64(1):18-24.
117. Ortorp A, Jonsson D, Mouhsen A, Vult von Steyern P. The fit of cobalt-chromium three-unit fixed dental prostheses fabricated with four different techniques: A comparative in vitro study. *Dent Mater.* 2011;27(4):356-63.
118. Groten M, Axmann D, Probster L, Weber H. Determination of the minimum number of marginal gap measurements required for practical in-vitro testing. *J Prosthet Dent.* 2000;83(1):40-9.
119. Sundar MK, Chikmagalur SB, Pasha F. Marginal fit and microleakage of cast and metal laser sintered copings--an in vitro study. *J Prosthodont Res.* 2014;58(4):252-8.
120. McLean JW, von Fraunhofer JA. The estimation of cement film thickness by an in vivo technique. *Br Dent J.* 1971;131(3):107-11.
121. Falk A, Vult von Steyern P, Fransson H, Thoren MM. Reliability of the impression replica technique. *Int J Prosthodont.* 2015;28(2):179-80.
122. Nakamura K, Mouhat M, Nergård JM, Lægread SJ, Kanno T, Milleding P, et al. Effect of cements on fracture resistance of monolithic zirconia crowns. *Acta Biomater Odontol Scand.* 2016;2(1):12-9.

123. Holst S, Karl M, Wichmann M, Matta RE. A new triple-scan protocol for 3D fit assessment of dental restorations. *Quintessence Int.* 2011;42(8):651-7.
124. Holmes JR, Sulik WD, Holland GA, Bayne SC. Marginal fit of castable ceramic crowns. *J Prosthet Dent.* 1992;67(5):594-9.
125. Leong D, Chai J, Lautenschlager E, Gilbert J. Marginal fit of machine-milled titanium and cast titanium single crowns. *Int J Prosthodont.* 1994;7(5):440-7.
126. Fransson B, Oilo G, Gjeitanger R. The fit of metal-ceramic crowns, a clinical study. *Dent Mater.* 1985;1(5):197-9.
127. McLean JW. Polycarboxylate cements. Five years' experience in general practice. *Br Dent J.* 1972;132(1):9-15.
128. Felton DA, Kanoy BE, Bayne SC, Wirthman GP. Effect of in vivo crown margin discrepancies on periodontal health. *J Prosthet Dent.* 1991;65(3):357-64.
129. Wilson PR. Effect of increasing cement space on cementation of artificial crowns. *J Prosthet Dent.* 1994;71(6):560-4.
130. Wu JC, Wilson PR. Optimal cement space for resin luting cements. *Int J Prosthodont.* 1994;7(3):209-15.
131. Son YH, Han CH, Kim S. Influence of internal-gap width and cement type on the retentive force of zirconia copings in pullout testing. *J Dent.* 2012;40(10):866-72.
132. Materials CoD, Devices. Revised american national standards institute/American dental association specification No. 8 for zinc phosphate cement. *J Am Dent Assoc.* 1978;96(1):121-3.
133. ISO. ISO Standard 9917-2 Dentistry -- Water-based cements -- Part 2: Resin-modified cements. Geneva, Switzerland: International Organization for Standardization; 2010.
134. Kane LM, Chronaios D, Sierralta M, George FM. Marginal and internal adaptation of milled cobalt-chromium copings. *J Prosthet Dent.* 2015;114(5):680-5.
135. Ishikiriyama A, Oliveira Jde F, Vieira DF, Mondelli J. Influence of some factors on the fit of cemented crowns. *J Prosthet Dent.* 1981;45(4):400-4.
136. Jørgensen KD. Factors affecting the film thickness of zinc phosphate cements. *Acta Odontol Scand.* 1960;18(4):479-90.
137. Fonseca JC, Henriques GE, Sobrinho LC, de Goes MF. Stress-relieving and porcelain firing cycle influence on marginal fit of commercially pure titanium and titanium-aluminum-vanadium copings. *Dent Mater.* 2003;19(7):686-91.
138. Han HS, Yang HS, Lim HP, Park YJ. Marginal accuracy and internal fit of machine-milled and cast titanium crowns. *J Prosthet Dent.* 2011;106(3):191-7.
139. Christensen GJ. Marginal fit of gold inlay castings. *J Prosthet Dent.* 1966;16(2):297-305.

140. Bronson MR, Lindquist TJ, Dawson DV. Clinical acceptability of crown margins versus marginal gaps as determined by predoctoral students and prosthodontists. *J Prosthodont.* 2005;14(4):226-32.
141. Cvar JF, Ryge G. Reprint of criteria for the clinical evaluation of dental restorative materials. 1971. *Clin Oral Investig.* 2005;9(4):215-32.
142. Ryge G, Jendresen M, Glantz P, Mjör I. Standardization of clinical investigators for studies of restorative materials. *Swed Dent J.* 1980;5(5-6):235-9.
143. Ryge G, Snyder M. Evaluating the clinical quality of restorations. *J Am Dent Assoc.* 1973;87(2):369-77.
144. Hickel R, Roulet JF, Bayne S, Heintze SD, Mjor IA, Peters M, et al. Recommendations for conducting controlled clinical studies of dental restorative materials. *Int Dent J.* 2007;57(5):300-2.
145. Dedmon H. Disparity in expert opinions on size of acceptable margin openings. *Oper Dent.* 1981;7(3):97-101.
146. Diaz-Arnold AM, Williams VD, Aquilino SA. The effect of film thickness on the tensile bond strength of a prosthodontic adhesive. *J Prosthet Dent.* 1991;66(5):614-8.
147. Keul C, Stawarczyk B, Erdelt KJ, Beuer F, Edelhoff D, Guth JF. Fit of 4-unit FDPs made of zirconia and CoCr-alloy after chairside and labside digitalization--a laboratory study. *Dent Mater.* 2014;30(4):400-7.
148. Park JK, Lee WS, Kim HY, Kim WC, Kim JH. Accuracy evaluation of metal copings fabricated by computer-aided milling and direct metal laser sintering systems. *J Adv Prosthodont.* 2015;7(2):122-8.
149. Quante K, Ludwig K, Kern M. Marginal and internal fit of metal-ceramic crowns fabricated with a new laser melting technology. *Dent Mater.* 2008;24(10):1311-5.
150. Xu D, Xiang N, Wei B. The marginal fit of selective laser melting-fabricated metal crowns: An in vitro study. *J Prosthet Dent.* 2014.
151. Ucar Y, Akova T, Akyil MS, Brantley WA. Internal fit evaluation of crowns prepared using a new dental crown fabrication technique: laser-sintered Co-Cr crowns. *J Prosthet Dent.* 2009;102(4):253-9.
152. Kim KB, Kim WC, Kim HY, Kim JH. An evaluation of marginal fit of three-unit fixed dental prostheses fabricated by direct metal laser sintering system. *Dent Mater.* 2013;29(7):e91-6.
153. Borba M, Cesar PF, Griggs JA, Della Bona A. Adaptation of all-ceramic fixed partial dentures. *Dent Mater.* 2011;27(11):1119-26.
154. Reich S, Wichmann M, Nkenke E, Proeschel P. Clinical fit of all-ceramic three-unit fixed partial dentures, generated with three different CAD/CAM systems. *Eur J Oral Sci.* 2005;113(2):174-9.
155. Huang Z, Zhang L, Zhu J, Zhang X. Clinical marginal and internal fit of metal ceramic crowns fabricated with a selective laser melting technology. *J Prosthet Dent.* 2015;113(6):623-7.

156. Nesse H, Ulstein DM, Vaage MM, Oilo M. Internal and marginal fit of cobalt-chromium fixed dental prostheses fabricated with 3 different techniques. *J Prosthet Dent.* 2015;114(5):686-92.
157. Klineberg I, Murray G. Design of superstructures for osseointegrated fixtures. *Swed Dent J Suppl.* 1985;28:63-9.
158. Jemt T. Failures and complications in 391 consecutively inserted fixed prostheses supported by Branemark implants in edentulous jaws: a study of treatment from the time of prosthesis placement to the first annual checkup. *Int J Oral Maxillofac Implants.* 1991;6(3):270-6.
159. Jemt T, Lekholm U, Adell R. Osseointegrated implants in the treatment of partially edentulous patients: a preliminary study on 876 consecutively placed fixtures. *Int J Oral Maxillofac Implants.* 1989;4(3):211-7.
160. Karl M, Winter W, Taylor TD, Heckmann SM. In vitro study on passive fit in implant-supported 5-unit fixed partial dentures. *Int J Oral Maxillofac Implants.* 2004;19(1):30-7.
161. de Torres EM, Rodrigues RC, de Mattos Mda G, Ribeiro RF. The effect of commercially pure titanium and alternative dental alloys on the marginal fit of one-piece cast implant frameworks. *J Dent.* 2007;35(10):800-5.
162. Carr AB, Stewart RB. Full-arch implant framework casting accuracy: preliminary in vitro observation for in vivo testing. *J Prosthodont.* 1993;2(1):2-8.
163. Hedkvist L, Mattsson T, Hellden LB. Clinical performance of a method for the fabrication of implant-supported precisely fitting titanium frameworks: a retrospective 5- to 8-year clinical follow-up study. *Clin Implant Dent Relat Res.* 2004;6(3):174-80.
164. Hellden L, Ericson G, Elliot A, Fornell J, Holmgren K, Nilner K, et al. A prospective 5-year multicenter study of the Cresco implantology concept. *Int J Prosthodont.* 2003;16(5):554-62.
165. Riedy SJ, Lang BR, Lang BE. Fit of implant frameworks fabricated by different techniques. *J Prosthet Dent.* 1997;78(6):596-604.
166. Ortorp A, Jemt T. Early laser-welded titanium frameworks supported by implants in the edentulous mandible: a 15-year comparative follow-up study. *Clin Implant Dent Relat Res.* 2009;11(4):311-22.
167. Al-Fadda SA, Zarb GA, Finer Y. A comparison of the accuracy of fit of 2 methods for fabricating implant-prosthetic frameworks. *Int J Prosthodont.* 2007;20(2):125-31.
168. Katsoulis J, Mericske-Stern R, Rotkina L, Zbaren C, Enkling N, Blatz MB. Precision of fit of implant-supported screw-retained 10-unit computer-aided-designed and computer-aided-manufactured frameworks made from zirconium dioxide and titanium: an in vitro study. *Clin Oral Implants Res.* 2014;25(2):165-74.

169. Ortorp A, Jemt T, Back T, Jalevik T. Comparisons of precision of fit between cast and CNC-milled titanium implant frameworks for the edentulous mandible. *Int J Prosthodont.* 2003;16(2):194-200.
170. Takahashi T, Gunne J. Fit of implant frameworks: an in vitro comparison between two fabrication techniques. *J Prosthet Dent.* 2003;89(3):256-60.
171. Abduo J, Lyons K, Bennani V, Waddell N, Swain M. Fit of screw-retained fixed implant frameworks fabricated by different methods: a systematic review. *Int J Prosthodont.* 2011;24(3):207.
172. Hjalmarsson L, Ortorp A, Smedberg JI, Jemt T. Precision of Fit to Implants: A Comparison of Cresco and Procera(R) Implant Bridge Frameworks. *Clin Implant Dent Relat Res.* 2010;12(4):271-80.
173. van Noort R. The future of dental devices is digital. *Dent Mater.* 2012;28(1):3-12.
174. Wismeijer D, Bragger U, Evans C, Kapos T, Kelly R, Millen C, et al. Consensus Statements and Recommended Clinical Procedures Regarding Restorative Materials and Techniques for Implant Dentistry. *Int J Oral Maxillofac Implants.* 2014;29(Suppl):137-40.
175. Kan JY, Rungcharassaeng K, Bohsali K, Goodacre CJ, Lang BR, Kan JY, et al. Clinical methods for evaluating implant framework fit. *J Prosthet Dent.* 1999;81(1):7-13.
176. Cheshire PD, Hobkirk JA. An in vivo quantitative analysis of the fit of Nobel Biocare implant superstructures. *J Oral Rehabil.* 1996;23(11):782-9.
177. Jemt T. In vivo measurements of precision of fit involving implant-supported prostheses in the edentulous jaw. *Int J Oral Maxillofac Implants.* 1996;11(2):151-8.
178. Papavassiliou H, Kourtis S, Katerelou J, Chronopoulos V. Radiographical evaluation of the gap at the implant-abutment interface. *J Esthet Restor Dent.* 2010;22(4):235-50.
179. Jemt T. Three-dimensional distortion of gold alloy castings and welded titanium frameworks. Measurements of the precision of fit between completed implant prostheses and the master casts in routine edentulous situations. *J Oral Rehabil.* 1995;22(8):557-64.
180. Clelland NL, Carr AB, Gilat A. Comparison of strains transferred to a bone simulant between as-cast and postsoldered implant frameworks for a five-implant-supported fixed prosthesis. *J Prosthodont.* 1996;5(3):193-200.
181. Karl M, Rosch S, Graef F, Taylor TD, Heckmann SM. Strain situation after fixation of three-unit ceramic veneered implant superstructures. *Implant Dent.* 2005;14(2):157-65.
182. Fernandez M, Delgado L, Molmeneu M, Garcia D, Rodriguez D. Analysis of the misfit of dental implant-supported prostheses made with three manufacturing processes. *J Prosthet Dent.* 2014;111(2):116-23.

183. Torsello F, di Torresanto VM, Ercoli C, Cordaro L. Evaluation of the marginal precision of one-piece complete arch titanium frameworks fabricated using five different methods for implant-supported restorations. *Clin Oral Implants Res.* 2008;19(8):772-9.
184. Koke U, Wolf A, Lenz P, Gilde H. In vitro investigation of marginal accuracy of implant-supported screw-retained partial dentures. *J Oral Rehabil.* 2004;31(5):477-82.
185. Tan KB, Rubenstein JE, Nicholls JI, Yuodelis RA. Three-dimensional analysis of the casting accuracy of one-piece, osseointegrated implant-retained prostheses. *Int J Prosthodont.* 1993;6(4):346-63.
186. Jemt T, Rubenstein JE, Carlsson L, Lang BR. Measuring fit at the implant prosthodontic interface. *J Prosthet Dent.* 1996;75(3):314-25.
187. Lie A, Jemt T. Photogrammetric measurements of implant positions. Description of a technique to determine the fit between implants and superstructures. *Clin Oral Implants Res.* 1994;5(1):30-6.
188. Bühler W. The method of least squares. Gauss: Springer; 1981. p. 138-41.
189. Eliasson A, Wennerberg A, Johansson A, Ortorp A, Jemt T. The Precision of Fit of Milled Titanium Implant Frameworks (I-Bridge(R)) in the Edentulous Jaw. *Clin Implant Dent Relat Res.* 2010;12(2):81-90.
190. Jemt T, Hjalmarsson L. In vitro measurements of precision of fit of implant-supported frameworks. A comparison between "virtual" and "physical" assessments of fit using two different techniques of measurements. *Clin Implant Dent Relat Res.* 2012;14 Suppl 1:e175-82.
191. Patterson E. Passive fit: Meaning, significance and assessment in relation to implant-supported prostheses. In: Naert I, editor. *Passive Fit of Implant-Supported Superstructures: Fiction or Reality*: Leuven University Press, Belgium; 1996. p. 17-28.
192. Sahin S, Cehreli MC. The significance of passive framework fit in implant prosthodontics: current status. *Implant Dent.* 2001;10(2):85-92.
193. Abduo J, Lyons K. Effect of vertical misfit on strain within screw-retained implant titanium and zirconia frameworks. *J Prosthodont Res.* 2012;56(2):102-9.
194. Abduo J, Lyons K, Waddell N, Bennani V, Swain M. A Comparison of Fit of CNC-Milled Titanium and Zirconia Frameworks to Implants. *Clin Implant Dent Relat Res.* 2012;14(1):e20-e9.
195. Smedberg JI, Nilner K, Rangert B, Svensson SA, Glantz SA. On the influence of superstructure connection on implant preload: a methodological and clinical study. *Clin Oral Implants Res.* 1996;7(1):55-63.
196. Kunavisarut C, Lang LA, Stoner BR, Felton DA. Finite element analysis on dental implant-supported prostheses without passive fit. *J Prosthodont.* 2002;11(1):30-40.
197. Duyck J, Ronold HJ, Van Oosterwyck H, Naert I, Vander Sloten J, Ellingsen JE. The influence of static and dynamic loading on

- marginal bone reactions around osseointegrated implants: an animal experimental study. *Clin Oral Implants Res.* 2001;12(3):207-18.
198. Duyck J, Vrielinck L, Lambrechts I, Abe Y, Schepers S, Politis C, et al. Biologic response of immediately versus delayed loaded implants supporting ill-fitting prostheses: an animal study. *Clin Implant Dent Relat Res.* 2005;7(3):150-8.
199. Jemt T, Lekholm U, Johansson CB. Bone response to implant-supported frameworks with differing degrees of misfit preload: in vivo study in rabbits. *Clin Implant Dent Relat Res.* 2000;2(3):129-37.
200. Carr AB, Gerard DA, Larsen PE. The response of bone in primates around unloaded dental implants supporting prostheses with different levels of fit. *J Prosthet Dent.* 1996;76(5):500-9.
201. Jemt T, Book K. Prosthesis misfit and marginal bone loss in edentulous implant patients. *Int J Oral Maxillofac Implants.* 1996;11(5):620-5.
202. Pjetursson BE, Bragger U, Lang NP, Zwahlen M. Comparison of survival and complication rates of tooth-supported fixed dental prostheses (FDPs) and implant-supported FDPs and single crowns (SCs). *Clin Oral Implants Res.* 2007;18:97-113.
203. Pjetursson BE, Tan K, Lang NP, Bragger U, Egger M, Zwahlen M. A systematic review of the survival and complication rates of fixed partial dentures (FPDs) after an observation period of at least 5 years. *Clin Oral Implants Res.* 2004;15(6):625-42.
204. Gemalmaz D, Alkumru HN. Marginal fit changes during porcelain firing cycles. *J Prosthet Dent.* 1995;73(1):49-54.
205. Felton DA, Sulik WD, Holland GA, Taylor DF, Bayne SC. Marginal discrepancy changes at various stages of construction of three-unit porcelain-fused-to-metal fixed partial dentures. *Dent Mater.* 1988;4(5):296-301.
206. Gemalmaz D, Berksun S, Kasapoglu C, Alkumru HN. Distortion of metal-ceramic fixed partial dentures resulting from metal-conditioning firing. *Quintessence Int.* 1996;27(3):193-201.
207. DeHoff PH, Anusavice KJ. Effect of metal design on marginal distortion of metal-ceramic crowns. *J Dent Res.* 1984;63(11):1327-31.
208. Buchanan WT, Svare CW, Turner KA. The effect of repeated firings and strength on marginal distortion in two ceramometal systems. *J Prosthet Dent.* 1981;45(5):502-6.
209. Shokry TE, Attia M, Mosleh I, Elhosary M, Hamza T, Shen C. Effect of metal selection and porcelain firing on the marginal accuracy of titanium-based metal ceramic restorations. *J Prosthet Dent.* 2010;103(1):45-52.
210. Richter-Snapp K, Aquilino SA, Svare CW, Turner KA. Change in marginal fit as related to margin design, alloy type, and porcelain proximity in porcelain-fused-to-metal restorations. *J Prosthet Dent.* 1988;60(4):435-9.

211. Zervas PJ, Papazoglou E, Beck FM, Carr AB. Distortion of three-unit implant frameworks during casting, soldering, and simulated porcelain firings. *J Prosthodont.* 1999;8(3):171-9.
212. Gemalmaz D, Berksun S, Alkumru HN, Kasapoglu C. Thermal cycling distortion of porcelain fused to metal fixed partial dentures. *J Prosthet Dent.* 1998;80(6):654-60.
213. Campbell SD, Sirakian A, Pelletier LB, Giordano RA. Effects of firing cycle and surface finishing on distortion of metal ceramic castings. *J Prosthet Dent.* 1995;74(5):476-81.
214. Campbell SD, Pelletier LB. Thermal cycling distortion of metal ceramics: Part II--Etiology. *J Prosthet Dent.* 1992;68(2):284-9.
215. Bridger DV, Nicholls JI. Distortion of ceramometal fixed partial dentures during the firing cycle. *J Prosthet Dent.* 1981;45(5):507-14.
216. Anusavice KJ, Carroll JE. Effect of incompatibility stress on the fit of metal-ceramic crowns. *J Dent Res.* 1987;66(8):1341-5.
217. Campbell SD, Pelletier LB. Thermal cycling distortion of metal ceramics: Part I--Metal collar width. *J Prosthet Dent.* 1992;67(5):603-8.
218. Tioosi R, Rodrigues RC, de Mattos Mda G, Ribeiro RF. Comparative analysis of the fit of 3-unit implant-supported frameworks cast in nickel-chromium and cobalt-chromium alloys and commercially pure titanium after casting, laser welding, and simulated porcelain firings. *Int J Prosthodont.* 2008;21(2):121-3.
219. de Vasconcellos LG, Buso L, Lombardo GH, Souza RO, Nogueira L, Jr., Bottino MA, et al. Opaque layer firing temperature and aging effect on the flexural strength of ceramic fused to cobalt-chromium alloy. *J Prosthodont.* 2010;19(6):471-7.
220. Hey J, Beuer F, Bense T, Boeckler AF. Single crowns with CAD/CAM-fabricated copings from titanium: 6-year clinical results. *J Prosthet Dent.* 2014;112(2):150-4.
221. Milleding P, Haag P, Neroth B, Renz I. Two years of clinical experience with Procera titanium crowns. *Int J Prosthodont.* 1998;11(3):224-32.
222. Nilson H, Bergman B, Bessing C, Lundqvist P, Andersson M. Titanium copings veneered with Procera ceramics: a longitudinal clinical study. *Int J Prosthodont.* 1994;7(2).
223. Tan K, Pjetursson BE, Lang NP, Chan ES. A systematic review of the survival and complication rates of fixed partial dentures (FPDs) after an observation period of at least 5 years. *Clin Oral Implants Res.* 2004;15:654-66.
224. Collett D. *Modelling survival data in medical research.* 2 ed. Boca Raton: Chapman & Hall/CRC; 2003. p. 15-28.
225. Heintze SD, Rousson V. Survival of zirconia- and metal-supported fixed dental prostheses: a systematic review. *Int J Prosthodont.* 2010;23(6):493-502.

226. Goodacre CJ, Bernal G, Rungcharassaeng K, Kan JY. Clinical complications in fixed prosthodontics. *J Prosthet Dent.* 2003;90:31-41.
227. Björklund MR, T. Utvärdering av passformsmätning mellan 3D-skanningstekniken och replikatekniken. [Bachelor's Essay]. In press 2015.
228. Flugge TV, Schlager S, Nelson K, Nahles S, Metzger MC. Precision of intraoral digital dental impressions with iTero and extraoral digitization with the iTero and a model scanner. *Am J Orthod Dentofacial Orthop.* 2013;144(3):471-8.
229. Henkel GL. A comparison of fixed prostheses generated from conventional vs digitally scanned dental impressions. *Compend Curr Educ Dentistry.* 2007;28(8):422-31.
230. Nedelcu RG, Persson AS. Scanning accuracy and precision in 4 intraoral scanners: an in vitro comparison based on 3-dimensional analysis. *J Prosthet Dent.* 2014;112(6):1461-71.
231. Nagrath R, Lahori M, Agrawal M. A Comparative Evaluation of Dimensional Accuracy and Surface Detail Reproduction of Four Hydrophilic Vinyl Polysiloxane Impression Materials Tested Under Dry, Moist, and Wet Conditions-An In Vitro Study. *J Indian Prosthodont Soc.* 2014;14(1):59-66.
232. Persson AS, Oden A, Andersson M, Sandborgh-Englund G. Digitization of simulated clinical dental impressions: virtual three-dimensional analysis of exactness. *Dent Mater.* 2009;25(7):929-36.
233. Ender A, Mehl A. Accuracy of complete-arch dental impressions: A new method of measuring trueness and precision. *J Prosthet Dent.* 2013;109(2):121-8.
234. Abduo J, Bennani V, Waddell N, Lyons K, Swain M. Assessing the fit of implant fixed prostheses: a critical review. *Int J Oral Maxillofac Implants.* 2010;25(3):506-15.
235. Matković T, Matković P, Malina J. Effects of Ni and Mo on the microstructure and some other properties of Co–Cr dental alloys. *J Alloy Compd.* 2004;366(1):293-7.
236. Lu Y, Wu S, Gan Y, Zhang S, Guo S, Lin J, et al. Microstructure, mechanical property and metal release of As-SLM CoCrW alloy under different solution treatment conditions. *J Mech Behav Biomed Mater.* 2015;55:179-90.
237. Lu Y, Wu S, Gan Y, Li J, Zhao C, Zhuo D, et al. Investigation on the microstructure, mechanical property and corrosion behavior of the selective laser melted CoCrW alloy for dental application. *Materials science & engineering C, Materials for biological applications.* 2015;49:517-25.
238. Hedberg YS, Qian B, Shen Z, Virtanen S, Wallinder IO. In vitro biocompatibility of CoCrMo dental alloys fabricated by selective laser melting. *Dent Mater.* 2014;30(5):525-34.

239. Xin X, Chen J, Xiang N, Gong Y, Wei B. Surface characteristics and corrosion properties of selective laser melted Co–Cr dental alloy after porcelain firing. *Dent Mater.* 2014;30(3):263-70.
240. Barbier L, Abeloos J, De Clercq C, Jacobs R. Peri-implant bone changes following tooth extraction, immediate placement and loading of implants in the edentulous maxilla. *Clin Oral Investig.* 2012;16(4):1061-70.
241. Kumar S, Sankara Narayanan TSN, Ganesh Sundara Raman S, Seshadri SK. Thermal oxidation of Ti6Al4V alloy: Microstructural and electrochemical characterization. *Mater Chem Phys.* 2010;119(1):337-46.
242. Guleryuz H, Cimenoglu H. Oxidation of Ti–6Al–4V alloy. *J Alloy Compd.* 2009;472(1):241-6.
243. Güçlü F, Çimenoğlu H, Kayalı E. The recrystallization and thermal oxidation behavior of CP-titanium. *Mater Sci Eng C.* 2006;26(8):1367-72.
244. Niu W, Bermingham MJ, Baburamani PS, Palanisamy S, Dargusch MS, Turk S, et al. The effect of cutting speed and heat treatment on the fatigue life of Grade 5 and Grade 23 Ti-6Al-4V alloys. *Mater Design.* 2013;46:640-4.
245. Kern M, Thompson VP. Effects of sandblasting and silica-coating procedures on pure titanium. *J Dent.* 1994;22(5):300-6.
246. van der Meer WJ, Andriessen FS, Wismeijer D, Ren Y. Application of intra-oral dental scanners in the digital workflow of implantology. *PLoS One.* 2012;7(8):e43312.
247. De Backer H, Van Maele G, Decock V, Van den Berghe L. Long-term survival of complete crowns, fixed dental prostheses, and cantilever fixed dental prostheses with posts and cores on root canal-treated teeth. *Int J Prosthodont.* 2007;20:229-34.
248. Libby G, Arcuri MR, LaVelle WE, Hebl L. Longevity of fixed partial dentures. *J Prosthet Dent.* 1997;78:127-31.
249. Karlsson S. The fit of Procera titanium crowns. An in vitro and clinical study. *Acta Odontol Scand.* 1993;51(3):129-34.
250. Kohorst P, Junghanns J, Dittmer MP, Borchers L, Stiesch M. Different CAD/CAM-processing routes for zirconia restorations: influence on fitting accuracy. *Clin Oral Investig.* 2011;15(4):527-36.
251. Jemt T, Lie A. Accuracy of implant-supported prostheses in the edentulous jaw: analysis of precision of fit between cast gold-alloy frameworks and master casts by means of a three-dimensional photogrammetric technique. *Clin Oral Implants Res.* 1995;6(3):172-80.
252. Katsoulis J, Mericske-Stern R, Enkling N, Katsoulis K, Blatz MB. In vitro precision of fit of computer-aided designed and computer-aided manufactured titanium screw-retained fixed dental prostheses before and after ceramic veneering. *Clin Oral Implants Res.* 2015;26(1):44-9.

253. Al-Turki LEE, Chai J, Lautenschlager E, Hutten M. Changes in prosthetic screw stability because of misfit of implant-supported prostheses. *Int J Prosthodont.* 2002;15(1):38-42.
254. Kallus T, Bessing C. Loose gold screws frequently occur in full-arch fixed prostheses supported by osseointegrated implants after 5 years. *Int J Oral Maxillofac Implants.* 1994;9(2):169-78.
255. Worthington P, Bolender C, Taylor T. The Swedish system of osseointegrated implants: problems and complications encountered during a 4-year trial period. *Int J Oral Maxillofac Implants.* 1987;2(2):77.
256. Zarb G, Schmitt A. The longitudinal clinical effectiveness of osseointegrated dental implants: the Toronto study. Part III: Problems and complications encountered. *J Prosthet dent.* 1990;64(2):185-94.
257. Abduo J, Judge R. Implications of implant framework misfit: a systematic review of biomechanical sequelae. *Int J Oral Maxillofac Implants.* 2014;29(3):608-21.
258. Bacchi A, Consani R, Mesquita M, Dos Santos M. Effect of framework material and vertical misfit on stress distribution in implant-supported partial prosthesis under load application: 3-D finite element analysis. *Acta Odontol Scand.* 2013;71(5):1243-9.
259. Jokstad A, Shokati B. New 3D technologies applied to assess the long-term clinical effects of misfit of the full jaw fixed prosthesis on dental implants. *Clin Oral Implants Res.* 2014.